

# Journal of Geophysical Research: Atmospheres

## RESEARCH ARTICLE

10.1002/2015JD023840

**Key Points:**

- July surface O<sub>3</sub> in the western U.S. is strongly correlated with meteorology
- July O<sub>3</sub> and NO<sub>2</sub> in the western U.S. increase with 500 hPa heights
- For emissions control evaluation, western U.S. O<sub>3</sub> trends should be corrected for meteorology

**Supporting Information:**

- Figures S1–S5

**Correspondence to:**

P. J. Reddy,  
preddyresearch@gmail.com

**Citation:**

Reddy, P. J., and G. G. Pfister (2016), Meteorological factors contributing to the interannual variability of midsummer surface ozone in Colorado, Utah, and other western U.S. states, *J. Geophys. Res. Atmos.*, 121, 2434–2456, doi:10.1002/2015JD023840.

Received 22 JUN 2015

Accepted 3 FEB 2016

Accepted article online 6 FEB 2016

Published online 10 MAR 2016

## Meteorological factors contributing to the interannual variability of midsummer surface ozone in Colorado, Utah, and other western U.S. states

**Patrick J. Reddy<sup>1,2</sup> and Gabriele G. Pfister<sup>3</sup>**

<sup>1</sup>Retired, <sup>2</sup>Visitor at the Atmospheric Chemistry Observations and Modeling Laboratory, NCAR, Boulder, Colorado, USA,  
<sup>3</sup>Atmospheric Chemistry Observations and Modeling Laboratory, NCAR, Boulder, Colorado, USA

**Abstract** We use daily maximum 8 h average surface O<sub>3</sub> concentrations (MDA8) for July 1995–2013, meteorological variables from the National Center for Environmental Prediction/National Center for Atmospheric Research Reanalysis, the North American Regional Reanalysis, and output from regional chemistry-climate simulations to assess relationships between O<sub>3</sub> and weather in the western U.S. We also explore relationships among July O<sub>3</sub>, satellite-derived NO<sub>2</sub>, and meteorology. A primary objective of this study is to identify an effective method for correcting the effects of meteorology on July MDA8. We find significant correlations between July MDA8 O<sub>3</sub> and meteorological variables for sites in or near Denver, Colorado, and Salt Lake City, Utah. The highest correlations were for 500 hPa heights, surface temperatures, and 700 hPa temperatures and zonal winds. We conclude that increased 500 hPa heights lead to high July O<sub>3</sub> in much of the western U.S., particularly in areas of elevated terrain near urban sources of NO<sub>2</sub> and other O<sub>3</sub> precursors. In addition to bringing warmer temperatures and fewer clouds, upper level ridges decrease winds and allow cyclic terrain-driven circulations to reduce transport away from sources. Because of strong, nearly linear responses of July MDA8 to 500 hPa heights, it is not reasonable to use uncorrected trends in peak O<sub>3</sub> for assessments of the effectiveness of emissions controls for much of the western U.S. Robust linear regressions for July MDA8 and tropospheric NO<sub>2</sub> with 500 hPa heights can be used to assess and correct trends in July MDA8 in the Intermountain West.

### 1. Introduction

Weather and climate have significant impacts on O<sub>3</sub> and its precursors, and interannual variations in meteorology can affect recent and future trends in O<sub>3</sub> and its precursors, including NO<sub>2</sub>. These effects can mask the true impacts of year-to-year changes in anthropogenic emissions. Understanding the relationships between the processes that are associated with O<sub>3</sub> formation and accumulation and meteorology can lead to improvements in modeling, forecasting, and the analyses of trends to assess the efficacy of emissions controls. We know that O<sub>3</sub> concentrations can increase with temperature as a result of peroxyacetyl nitrate (PAN) photochemistry and increases in biogenic emissions [Sillman and Samson, 1995]. Recent research has also shown strong correlations between surface O<sub>3</sub> concentrations and surface temperatures in the eastern U.S. [Bloomer et al., 2009; Camalier et al., 2007]. Other studies have explored the relationships between O<sub>3</sub> and relative humidity, winds, and soil moisture-atmosphere coupling regimes [Davis et al., 2011; Tawfik and Steiner, 2013].

In addition, Ellis et al. [2000] and MacDonald et al. [2001] found that high O<sub>3</sub> in the southwestern U.S. was associated with the presence of a 500 hPa ridge. While shallow mixed layers have been found to be conducive to high O<sub>3</sub> over much of the U.S., Wise and Comrie [2005] and White et al. [2007] found that O<sub>3</sub> in the southwestern U.S. and in New England increased with increasing planetary boundary layer (PBL) heights. White et al. [2007] point out that the increases in mixing heights during high-O<sub>3</sub> events in New England may be due to the ensemble of favorable meteorological conditions that also occur during high-O<sub>3</sub> events. These include higher temperatures, reduced cloud cover, strong insolation, and lighter winds. These are factors that are also associated with upper level high-pressure systems and increased 500 hPa heights. Seidel et al. [2012] found that at most locations (but not at some coastal locations), seasonal variability of daytime PBL heights tends to be positively correlated with both surface temperatures and 500 hPa heights and that mean summer afternoon PBL heights were well over 2 km above ground level for most of the inland western U.S. Clearly, large PBL heights in the western U.S. are associated with high-pressure systems, and

these usher in other conditions conducive to high O<sub>3</sub> concentrations. The question arises whether deep vertical mixing itself, however, contributes to high O<sub>3</sub> in the western U.S.

Large PBL heights may make it possible for elevated residual layers [Zhang and Rao, 1999; McKendry and Lundgren, 2000], O<sub>3</sub> from thunderstorms, pollutants injected into the free troposphere by terrain [Langford et al., 2010; Henne et al., 2004], O<sub>3</sub> transported over larger scales, and mountain-plains solenoid circulations [Wolyn and Mckee, 1994] to contribute to surface O<sub>3</sub> concentrations. Dosio et al. [2002], for example, found that cyclic mountain-plains circulations over the Po Valley and nearby mountains that occur when synoptic-scale forcing is weak (as is the case under the influence of a strong 500 hPa high) lead to the long-term, local persistence of a passive tracer introduced into a mesoscale model of local flows. They also concluded that this persistence and the potential for recirculation and reentrainment of residual layers aloft favored a net buildup of O<sub>3</sub> on the order of 10 ppb d<sup>-1</sup>.

Soil moisture conditions in the western U.S. can modulate the strength and extent of mountain-plains circulations and affect how much influence these systems have on local O<sub>3</sub>. Drought, which can be a consequence of persistent upper level high pressure in the western U.S., can lead to deeper vertical mixing and stronger mountain-plains circulations. This is because lower soil moisture associated with drought causes reductions in the surface latent heat flux and subsequent increases in soil and surface temperatures. These increases give rise to deeper boundary layer growth during the day [Zhou and Geerts, 2012; Pan and Mahrt, 1987; Ek and Holtslag, 2004], higher mean temperatures within the PBL, and a greater potential for thermally driven winds.

We focus on the month of July when surface O<sub>3</sub> levels typically peak in the western U.S. Our initial objective is to identify the key monthly mean July meteorological variables that affect interannual variations in July daily maximum 8 h average surface O<sub>3</sub> concentrations (MDA8) in the western U.S. and to identify one or more that best predict year-to-year variations in July MDA8. We examine variables that have the greatest correlations with July MDA8 and the role of terrain-driven circulations under persistent 500 hPa high-pressure systems.

Although the primary focus of this study is relationships between O<sub>3</sub> and meteorology in the Front Range and Wasatch Front urban corridors of Colorado and Utah, we also briefly consider relationships between O<sub>3</sub> and 500 hPa heights for a broader region of the western U.S. The analysis for a wider region underscores the geographic extent of high correlations with 500 hPa heights and the possible role of elevation. Monthly mean 500 hPa heights may be a useful surrogate for O<sub>3</sub>-meteorology relationships in many other areas of the western U.S.

We also consider relationships between July Ozone Monitoring Instrument (OMI) tropospheric NO<sub>2</sub> and 500 hPa heights and MDA8 in Colorado and Utah, states where the correlations between O<sub>3</sub> and 500 hPa heights are generally the strongest, terrain-driven circulations are widespread, and the summer mixed layer is deep. Finally, we show that the relationships with 500 hPa heights can be used to correct trends in July MDA8 and OMI tropospheric NO<sub>2</sub> for the effects of year-to-year changes in meteorology.

## 2. Data Sources and Methods

### 2.1. Data Sources

We used the following data products in our analysis. Data for the July MDA8 for available years (1995 through 2013) for 90 sites in the western portions of the U.S. (bounded by 29–49°N and 122–94°W) were acquired from the Environmental Protection Agency (EPA) Air Quality System (AQS). The boundaries of the study area were selected based on a desire to highlight O<sub>3</sub>-meteorology relationships in the Rocky Mountain states, nearby plains, and Intermountain West and to provide some indication of where patterns unique to these regions might begin to shift. In many areas of the northwestern United States, long-term O<sub>3</sub> time series were not available. In order to be included in the analysis, each site had to have a minimum of 8 years of data, and some sites had all 19 years of the 1995–2013 study period. Surface O<sub>3</sub> monitor sites were classified as urban, suburban, rural/suburban, or rural based on a subjective or qualitative interpretation of aerial imagery for each site. This classification proved useful for assessing the strength of elevation effects on correlations with meteorology.

Surface O<sub>3</sub> data were correlated with a variety of meteorological variables from two reanalysis data sets, the National Center for Environmental Prediction/National Center for Atmospheric Research (NCEP/NCAR)

Reanalysis [Kalnay *et al.*, 1996] and the North American Regional Reanalysis (NARR) [Mesinger *et al.*, 2006]. The meteorological variables considered include mean 500 hPa heights, mean surface temperatures, mean surface scalar wind speeds, mean PBL heights, mean soil moisture, mean 700 hPa temperatures, and mean 700 hPa zonal and meridional winds. These variables represent a subset of a larger list that was initially screened, and they were selected because of their expected association with conditions that affect O<sub>3</sub> formation and accumulation.

Both the NCEP/NCAR Reanalysis and NARR provide consistent, high-quality meteorological and climate data based on forecast and analysis models coupled with comprehensive observational data assimilation. The NCEP/NCAR Reanalysis data set conforms to a grid size of 2.5° by 2.5°, and the NARR has a grid spacing of 32 km. While neither the NCEP/NCAR Reanalysis nor the NARR have sufficient spatial resolution to fully capture the details of mesoscale variations affected by complex local terrain, they can in some cases provide a better spatial representation of mean meteorological conditions affecting O<sub>3</sub> photochemistry over the course of a day than data for a single point. Along Colorado's Front Range, for example, mean conditions for heights and temperatures for a typical summer mountain-plains diurnal recirculation of O<sub>3</sub> and its precursors may be reasonably represented by data for a single 2.5° by 2.5° grid cell which covers much of the spatial domain of the circulation itself. Figure S1 in the supporting information shows the NCEP/NCAR Reanalysis grid cell over Denver, Colorado, which includes the Front Range Region, the high mountains west of Denver, and the Platte Valley which widens between Denver and Greeley.

July mean surface O<sub>3</sub> data were also correlated with OMI tropospheric NO<sub>2</sub> and OMI tropospheric NO<sub>2</sub> data were linearly regressed against 500 hPa heights from the NCEP/NCAR Reanalysis in an effort to characterize interrelationships among O<sub>3</sub>, NO<sub>2</sub>, and climate. The OMI NO<sub>2</sub> data used were Version 2.1 Level 3 data cloud-screened at 30% with a grid resolution of 0.25° by 0.25° based on the NASA algorithm [Bucsela *et al.*, 2013]. While many factors affect the accuracy of OMI NO<sub>2</sub> retrievals, they have been found to generally agree with other NO<sub>2</sub> measurements to within ±20% [Lamsal *et al.*, 2014].

The relationships between mean July MDA8 and meteorological variables were also tested on model results from a regional fully coupled chemistry-transport model. The Nested Regional Climate Model (NRCM) with chemistry (NRCM-Chem) is based on the regional Weather and Forecasting model (WRF) with Chemistry (WRF-Chem, version 3.3) and has been updated to include climate-relevant processes and feedbacks. We simulated air quality over the summertime U.S. for present and a 2050 future time period at high spatial resolution (12 km grid spacing) under the Special Report on Emissions Scenarios A2 climate and Representative Concentration Pathway leading to 8.5 W/m<sup>2</sup> warming by 2100 (RCP8.5) anthropogenic precursor emission scenario. A brief description of the model simulations and setup is presented here. For a more detailed description and analysis, the reader is referred to Pfister *et al.* [2014].

The meteorological initial (IC) and boundary conditions (BC) are based on global simulations from the Community Climate System Model (CCSM 3.0), which were dynamically downscaled to a 36 × 36 km<sup>2</sup> domain over the larger North America region [Done *et al.*, 2013]. Chemical IC and BC are based on chemistry-climate simulations from the global Community Atmosphere Model with Chemistry (CAM-Chem) for a comparable climate and anthropogenic emission scenario. Anthropogenic emission inputs for present and future time periods at high resolution were developed by regridding the global RCP emissions [Lamarque *et al.*, 2011] included in the CAM-Chem simulations from 0.5° to 0.1° using the finer 0.1° spatial information from Emission Database for Global Atmospheric Research version 4.1 (<http://edgar.jrc.ec.europa.eu>). For fire emissions we created an annual hourly climatology based on fire emissions for 2002–2010 from the NCAR Fire model FINN [Wiedinmyer *et al.*, 2011].

Three sets of simulations were conducted each for 13 climatological summers: a present time base simulation, a future time simulation centered around 2050 with future climate and future anthropogenic emission projections (reduced O<sub>3</sub> precursor emissions over the U.S.), and a second future time simulation, which simulates future climate and global emissions changes, i.e., has future meteorological and chemical IC and BC, but uses present time anthropogenic precursor emissions over the regional domain. In this paper, we will refer to these as the Present Era, Future, and Future A scenarios, respectively. Modeled surface O<sub>3</sub> over the U.S. during the Present Era was evaluated by comparison to hourly O<sub>3</sub> measurements from the EPA air quality monitoring network [Pfister *et al.*, 2014]. It was shown that the model is capable of representing well the observed diurnal cycle and also captures the observed variability in hourly summertime surface ozone.

Monthly mean MDA8 O<sub>3</sub> concentrations were calculated from hourly surface O<sub>3</sub> model data and used in the current analysis. Monthly mean 500 hPa height levels were derived from 6-hourly output. Simulations for these three eras are used to shed light on relationships between O<sub>3</sub> and NO<sub>2</sub> and local sources and circulations. Trends in future concentrations are not the focus of our study.

## 2.2. Methods

Monthly mean MDA8 values were calculated and analyzed at each monitoring site for July, a peak month for both O<sub>3</sub> and atmospheric temperatures at many locations in the western U.S. July monthly mean values for MDA8 and meteorological variables were chosen for a variety of reasons. Our initial focus was on Colorado where we found that there were increasingly higher correlations between MDA8 and 500 hPa heights as averaging times increased from 1 day to 30 days. We calculated Pearson correlation coefficients for 1, 2, 3, 5, 10, 20, and 30 day moving averages of MDA8 O<sub>3</sub> and NCEP/NCAR Reanalysis 500 hPa heights for June through August of 2003 at Rocky Flats North (RFLAT, 27 km northwest of downtown Denver, Colorado). The correlation for 1 day averages was 0.54 and the correlation peaked for the roughly sixty 30 day moving averages with a value of 0.98. Second, the use of monthly means is expected to reduce the influence of day-to-day variations in synoptic and mesoscale meteorology on O<sub>3</sub> [Rasmussen *et al.*, 2012] and to provide a simple basis for correcting long-term trends in O<sub>3</sub> for the effects of weather using readily available data. Such corrected trends provide a better measure of the impacts of precursor emissions controls. We also performed statistical analyses for other summer months and found that correlations between monthly summer MDA8 and 500 hPa heights for RFLAT for 1995–2013 peaked in July with Pearson correlations of 0.57, 0.92, and 0.43, for June, July, and August, respectively.

There were additional, compelling reasons for selecting means for July over any other metric such as the 3 year average of the annual fourth maximum MDA8, which is used by the U.S. EPA to determine compliance with the federal standard for O<sub>3</sub>. The latter value represents the tail of the distribution for MDA8 and is more likely to be influenced by atypical meteorology not well represented by a monthly mean. For example, while 86% of the 1995–2013 variance in July monthly mean MDA8 at RFLAT is explained by July mean 500 hPa, only 60% and 41% of the variance in the annual fourth maximum is explained by July mean 500 hPa heights and June through August mean 500 hPa heights, respectively. July mean MDA8 values were retained for the analyses for years with at least 24 days of valid data.

A primary objective of this study is to identify an effective method for interpreting and correcting the effects of meteorology on July MDA8. In Colorado, Utah, and Wyoming, both the correlation coefficients and R<sup>2</sup> values for linear regressions between July mean 500 hPa heights and July mean MDA8 are generally higher than those for pairings between mean MDA8 and other meteorological variables (section 3). The relationship between July mean MDA8 and 500 hPa heights is ultimately used in this study to estimate trends in O<sub>3</sub>, adjusted for the effects of average weather (section 6.2).

Correlation coefficients were calculated for July mean MDA8 and July mean values of 500 hPa heights, surface temperature, 700 hPa temperature, 700 hPa meridional wind, and 700 hPa zonal winds from the NCEP/NCAR Reanalysis. July mean MDA8 was linearly regressed against July mean values of 700 hPa temperature, 700 hPa meridional winds, 700 hPa zonal winds, and 500 hPa heights. July MDA8 values were removed from the analyses if studentized residuals from regressions against 500 hPa heights were greater than or equal to 3.0, except in cases where multiple sites had anomalous values in the same year, there were reasons to believe that the outliers could represent regional phenomena, or removal had negligible effects on the slope and R<sup>2</sup>. The resulting R<sup>2</sup> values for 90 sites were regressed against site elevations, and sites not classified as rural were also considered separately.

O<sub>3</sub> concentrations and 500 hPa heights for July were high in 2002, 2003, 2006, and 2012 and low in 1995, 1997, 2004, and 2009 in most of Colorado. Composites or means of NARR 500 hPa heights and differences in NARR surface scalar wind speeds, NARR surface soil moisture, and NARR PBL heights for these two groups of years were compared in order to assess the influences of meteorology on O<sub>3</sub>. We also examined Global Precipitation Climatology Centre version 6 (GPCC v6) precipitation anomalies (with respect to 1981–2010 norms), National Lightning Detection Network (NLDN) ground strikes, and the Oceanic Niño Index (ONI, a widely used El Niño–Southern Oscillation (ENSO) index) for these two groups. Both the monthly precipitation and NLDN data were used to assess possible influences of regional July precipitation patterns and thunderstorms on O<sub>3</sub>. The GPCC v6 data used have a resolution of 1° by 1° based on more than 9000 North American

**Table 1.** Pearson Correlation Coefficients for July MDA8 O<sub>3</sub> and July Mean NCEP/NCAR Reanalysis Variables for 1995–2013 for Select Sites in Colorado, Wyoming, and Utah<sup>a</sup>

Site Name	Latitude	Longitude	State	500 hPa Heights	Surface Temperatures	700 hPa Temperatures	700 hPa Meridional Winds	700 hPa Zonal Winds
Air Force Academy (AFA)	38.958	-104.817	CO	0.64	<b>0.73</b>	<b>0.74</b>	0.12	-0.64
Arvada (ARV)	39.801	-105.099	CO	<b>0.78</b>	0.76	<b>0.77</b>	0.06	-0.76
Carriage (CRG)	39.752	-105.031	CO	<b>0.91</b>	0.88	0.87	0.20	<b>-0.94</b>
Chatfield Reservoir (CHAT)	39.538	-105.065	CO	<b>0.84</b>	0.73	<b>0.77</b>	-0.09	-0.74
Fort Collins (FTC)	40.576	-105.079	CO	<b>0.76</b>	<b>0.68</b>	0.64	0.15	-0.58
Gothic (GOTH)	38.957	-106.985	CO	<b>0.57</b>	0.54	<b>0.66</b>	-0.06	-0.32
Greeley (GRE)	40.416	-104.692	CO	<b>0.81</b>	0.73	<b>0.74</b>	0.16	-0.63
Highlands Ranch (HLD)	39.569	-104.957	CO	<b>0.92</b>	0.76	<b>0.84</b>	0.17	-0.55
Niwot Ridge Tundra (NWRT)	40.050	-105.590	CO	0.75	<b>0.78</b>	<b>0.87</b>	0.18	-0.75
NREL (NREL)	39.742	-105.179	CO	<b>0.90</b>	0.80	0.79	0.17	<b>-0.86</b>
Rocky Flats (RFLAT)	39.913	-105.188	CO	<b>0.92</b>	0.77	0.77	0.12	<b>-0.92</b>
Rocky Mountain National Park (RMNP)	40.277	-105.545	CO	0.76	0.77	<b>0.78</b>	0.20	<b>-0.96</b>
South Boulder Creek (SBC)	39.957	-105.238	CO	<b>0.83</b>	0.71	0.71	0.11	<b>-0.94</b>
Centennial (CEN)	41.364	-106.240	WY	<b>0.75</b>	0.71	<b>0.75</b>	0.09	<b>-0.80</b>
Brigham City (BRG)	41.493	-112.019	UT	0.78	<b>0.84</b>	<b>0.79</b>	-0.49	-0.73
Cottonwood (COT)	40.647	-111.850	UT	<b>0.77</b>	0.72	<b>0.77</b>	-0.62	-0.57
Harrisville (HAR)	41.304	-111.988	UT	0.78	<b>0.84</b>	<b>0.88</b>	-0.46	-0.69
Highland (HIGH)	40.903	-111.884	UT	<b>0.64</b>	0.46	0.54	-0.32	<b>-0.56</b>
Logan (LOG)	41.731	-111.838	UT	0.62	<b>0.76</b>	0.74	-0.25	<b>-0.84</b>
North Provo (NPRO)	40.254	-111.663	UT	<b>0.86</b>	0.80	<b>0.84</b>	-0.81	-0.42
Salt Lake City Hawthorne (SLCH)	40.736	-111.872	UT	<b>0.89</b>	0.76	<b>0.78</b>	-0.69	-0.57
Salt Lake City Lakepoint (SLCL)	40.736	-112.210	UT	<b>0.60</b>	0.52	0.56	-0.35	<b>-0.74</b>
Spanish Fork (SPAN)	40.136	-111.661	UT	<b>0.73</b>	0.69	<b>0.73</b>	-0.58	-0.46
Site means				<b>0.77</b>	0.73	<b>0.75</b>	-0.13	-0.69

<sup>a</sup>Highest two correlations for each site are underlined and in bold; ties are also in italics.

stations for much of the period of interest [Becker *et al.*, 2013; Schneider *et al.*, 2014; Schneider *et al.*, 2011], and the NLDN data are in ground strikes per 4 km<sup>2</sup>. While this data set may not capture all of the local-scale impacts of storms on O<sub>3</sub>, we expect that it serves as a useful indicator of the effects of summer precipitation regimes on O<sub>3</sub>.

Residuals from the regressions of July MDA8 and 500 hPa heights and OMI tropospheric NO<sub>2</sub> and 500 hPa heights were used to determine trends in July mean MDA8 and NO<sub>2</sub> after correction for the effects of weather or climate. Trends were calculated for two regions with the strongest relationships between O<sub>3</sub> and 500 hPa heights. The first of these was based on 14 Colorado Front Range sites including Colorado Springs, Denver, Boulder, Fort Collins, Greeley, and nearby foothills and mountain sites east of the Continental Divide. The trend for the second region, the Utah Wasatch Front, was based on nine sites including Salt Lake City, Brigham City, Logan, and Bountiful.

### 3. Statistical Relationships Between July Mean MDA8 O<sub>3</sub> and NCEP/NCAR Reanalysis Variables

We calculated Pearson correlations between July MDA8 O<sub>3</sub> and NCEP/NCAR variables (500 hPa heights, surface temperatures, 700 hPa temperatures, and 700 hPa meridional and zonal winds) for select monitoring sites in Colorado, Wyoming, and Utah. These three states include some of the highest correlations between July MDA8 and meteorological variables, some of the highest and most complex terrain in the region, and large urban areas centered on Salt Lake City, Utah, and Denver, Colorado. The results for 23 sites in these three states are presented in Table 1. All of these sites are in or near the Denver and Salt Lake City areas, including Centennial, Wyoming, which is about 200 km northwest of Denver. The highest correlations are for 500 hPa heights (with a mean of 0.77), surface temperatures (with a mean of 0.73), 700 hPa temperatures (with a mean of 0.75), and 700 hPa zonal winds (with a mean of -0.69).

As we discussed in section 1, it makes sense that 500 hPa heights have a strong, positive correlation with O<sub>3</sub>, since high heights are associated with many of the meteorological conditions conducive to high O<sub>3</sub>,

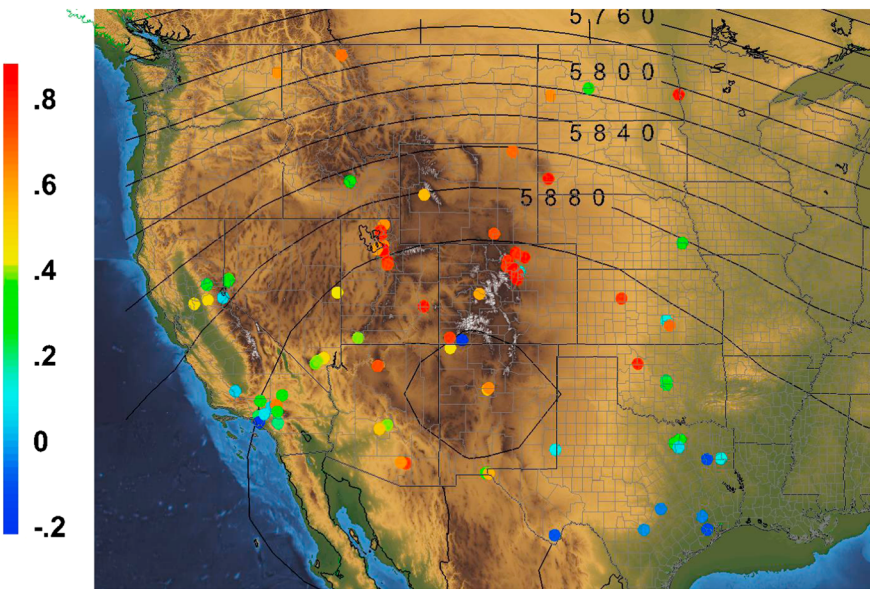


**Figure 1.** Map of Pearson correlation coefficients for mean July MDA8 O<sub>3</sub> and NCEP/NCAR Reanalysis 500 hPa heights for available data from 1995 to 2013 and contours of July mean NCEP/NCAR Reanalysis 500 hPa heights for this period.

including clear skies, high surface temperatures, light winds, and a shift from more energetic synoptically driven transport and dispersion to local and regional circulations. In addition, peak afternoon mixing heights in many of the high-altitude sites in the study area extend to the 500 hPa level or higher. Consequently, the 500 hPa height variable provides a measure of the mean temperatures in the afternoon mixed layer in many of these areas, since 500 hPa heights are directly affected by temperatures in the atmospheric column.

The highest correlations with 500 hPa heights in these three states are at sites in the Colorado Front Range (0.91 at CRG, 0.84 at CHAT, 0.81 at GRE, 0.92 at HLD, 0.90 at NREL, 0.92 at RFLAT, and 0.83 at SBC) and Utah (0.86 at NPRO and 0.89 at SLCH). Even the lowest correlations are greater than 0.6. Correlations with temperatures at 700 hPa and the surface are slightly lower than correlations between O<sub>3</sub> and 500 hPa heights. O<sub>3</sub> is significantly anticorrelated with 700 hPa zonal winds at most sites listed in Table 1 and significantly anticorrelated with 700 hPa meridional winds at most sites in Utah. For sites in Colorado and Wyoming, this suggests that O<sub>3</sub> concentrations increase with reduced westerly or increased easterly flows in this region. We will discuss the relationships between decreased zonal flow aloft and mountain-plains circulations in Colorado later (sections 4.1 and 5). Similarly, in the Salt Lake City region, thermally driven upslope, lake breeze, and mountain-plains circulations produce southward surface flows in the afternoon as far as 50 km to the south of the Great Salt Lake in summer [Stewart *et al.*, 2002]. Thus, an increase in meridional flows at 700 hPa might be expected to disrupt these terrain-driven circulations that are likely associated with the highest O<sub>3</sub> concentration events.

We show the Pearson correlation coefficients for July MDA8 O<sub>3</sub> and 500 hPa heights for all 90 sites considered in this study and the topography of the Western U.S. in Figure 1. Mean July 500 hPa height contours for 1995–2013 in Figure 1 show a mean upper level high-pressure system centered over New Mexico. The highest correlations tend to be clustered in Utah, Colorado, Arizona, Wyoming, North and South Dakota, and western portions of Kansas and Oklahoma. It is possible that somewhat lower correlations found to the south and west of the high-pressure center are due to increased clouds and precipitation. The lowest correlations, which in some cases were negative, are located in California, most of Texas, and an isolated portion of southwest Colorado. Structural differences in the atmosphere at these locations (e.g., the typical depth of the PBL and flow patterns), differences in the timing of peak O<sub>3</sub> during the year, and the relative impacts of precursor emissions trends in each area can affect these correlations.

We also derived least squares linear regressions for July MDA8 O<sub>3</sub> and select NCEP/NCAR variables. First, we completed regressions between July MDA8 and surface temperatures for sites in Colorado and Utah in order to compare historical rates of change with published results for the eastern and western U.S. We calculated

**Table 2.**  $R^2$  Values for Linear Regressions Between July MDA8 O<sub>3</sub> and July Mean NCEP/NCAR Reanalysis Variables for 1995–2013, Years of Data Used, Mean July MDA8, Site Classification, and Elevation for Select Sites in Colorado, Wyoming, and Utah<sup>a</sup>

Site	July Mean 700 hPa Temperatures	July Mean 700 hPa Meridional Winds	July Mean 700 hPa Zonal Winds	July Mean 500 hPa Heights	Years of Data	Mean July MDA8 (ppb)	Classification	Elevation (m)
AFA	<b>0.55</b>	(0.01)	0.21	0.41	18	57.4	suburban	1970
ARV	0.59	(0.00)	0.33	<b>0.60</b>	17	59.4	suburban	1638
CRG	0.76	(0.04)	0.43	<b>0.82</b>	18	58.0	urban	1620
CHAT	0.59	(0.01)	0.39	<b>0.71</b>	18	66.2	rural/suburban	1678
FTC	0.41	(0.02)	0.45	<b>0.57</b>	18	53.5	urban	1522
GOTH	<b>0.44</b>	(0.00)	0.09	0.33	18	53.5	rural	2916
GRE	0.55	(0.03)	0.37	<b>0.65</b>	19	61.1	suburban	1423
HLD	0.70	(0.03)	0.31	<b>0.84</b>	17	63.4	suburban	1741
NWRT	<b>0.75</b>	(0.03)	0.43	0.56	9	60.3	rural	3538
NREL	0.62	(0.03)	0.39	<b>0.81</b>	19	65.7	rural/suburban	1831
RFLAT	0.60	(0.02)	0.48	<b>0.86</b>	19	66.0	rural/suburban	1800
RMNP	<b>0.61</b>	(0.04)	0.34	0.57	18	60.1	rural	2738
SBC	0.50	(0.01)	0.55	<b>0.68</b>	19	59.9	rural/suburban	1669
CEN	<b>0.57</b>	(0.01)	0.14	<b>0.57</b>	19	57.7	rural	3173
BRG	<b>0.63</b>	(0.24)	0.39	0.60	13	61.7	urban	1330
COT	0.59	0.38	0.37	<b>0.60</b>	14	64.8	urban	1332
HAR	<b>0.78</b>	(0.21)	0.41	0.60	12	64.1	urban	1318
HIGH	0.29	(0.10)	0.35	<b>0.40</b>	16	63.7	urban	1309
LOG	<b>0.55</b>	(0.06)	0.28	0.39	13	58.2	urban	1381
NPRO	0.71	0.66	0.21	<b>0.73</b>	19	60.6	urban	1403
SLCH	0.60	0.48	0.39	<b>0.79</b>	17	62.1	urban	1304
SLCL	0.31	(0.13)	0.19	<b>0.36</b>	19	61.8	urban	1279
SPAN	<b>0.53</b>	0.33	0.13	<b>0.53</b>	16	62.2	rural/suburban	1381
<b>Site means</b>	0.58	0.12	0.33	<b>0.61</b>	16.7	60.9		1795

<sup>a</sup>Highest  $R^2$  values are underlined and in bold, ties are also in italics, and the null hypothesis for the slope of regressions with 500 hPa heights ( $p = 0.05$ ) is rejected in all cases except where  $R^2$  value is in parentheses.

mean increases of 3.3 and 3.0 ppb K<sup>-1</sup> in July MDA8 at 14 Colorado Front Range and 9 Utah Wasatch Front sites, respectively, for 1995–2013. These can be compared with 2.2–3.2 ppb K<sup>-1</sup> for hourly O<sub>3</sub> [Bloomer et al., 2009] and 3–6 ppb K<sup>-1</sup> for MDA8 [Rasmussen et al., 2012] for the eastern U.S., and 1.8–4.6 ppb K<sup>-1</sup> for hourly O<sub>3</sub> at sites in California in the 1990s and 2000s [Steiner et al., 2010].

Next, we examined linear regressions for four other NCEP/NCAR variables highly correlated with O<sub>3</sub>: July mean 700 hPa temperatures, 700 hPa meridional and zonal winds, and 500 hPa heights. Table 2 provides these results for the 23 sites in Colorado, Wyoming, and Utah. The years of data used for each site, the July mean MDA8 O<sub>3</sub>, a qualitative land use classification, and the elevation of each site in meters are also listed.

$R^2$  values are generally highest for 500 hPa heights with a mean of 0.61. Regressions against 700 hPa temperatures have a mean  $R^2$  of 0.58, and regressions against July 700 hPa meridional and zonal winds have mean  $R^2$  values of 0.12 and 0.33, respectively. The highest  $R^2$  for regressions against 500 hPa heights are along Colorado's Front Range with 0.82 at CRG, 0.84 at HLD, 0.81 at NREL, and 0.86 at RFLAT.

Similar high  $R^2$  values (0.56 to 0.80) are reported by Camalier et al. [2007] who developed a generalized linear multivariable model for MDA8 for 39 sites in the eastern U.S. based on meteorology. Their model is derived from daily data for May through September. Geopotential heights and data for the 700 and 500 hPa levels did not survive their initial screening. It is unclear whether the differences between our results and theirs are related to the differences in averaging times (recall that correlations between RFLAT MDA8 and 500 hPa heights were lowest for 1 day averages), differences in seasons (July versus May through September), structural differences in the atmosphere (e.g., mean afternoon mixing heights are much higher in much of the western U.S.), or some combination of these and other factors.

Plots of linear regressions between July MDA8 and July 500 hPa heights for RFLAT, CRG, GOTH, and SLCH are presented with confidence limits in Figure 2; in each case the null hypothesis is rejected ( $p = 0.05$ ). These plots show that a linear model provides a reasonable approximation of the response of July MDA8 to 500 hPa heights. July of 2003 was high for both O<sub>3</sub> and 500 hPa heights at each site depicted in Figure 2, but it was

not identified as an outlier for any of these sites. Data points for 2003, however, have substantial influence on the regressions in each plot because they are endpoints on the regression line. Residual values are low for each case but GOTH (which is 191 km southwest of Denver near Aspen), where July of 2003 had a relatively high residual of 2.8 ppb.

Wildfire smoke originating in Asia/Siberia caused significant increases in North American CO and O<sub>3</sub> concentrations during the summer of 2003 [Jaffe *et al.*, 2004; Bertschi and Jaffe, 2005]. Interrelationships among wildfire frequency and extent, meteorology, smoke, and O<sub>3</sub> are complex [Jaffe and Wigder, 2012; Zhang *et al.*, 2014b]. Wildfires increase in size and frequency during drought conditions, and drought conditions in the western U.S. are associated with persistent 500 hPa ridges. Is the response of O<sub>3</sub> to increased heights, therefore, partly due to the effects of wildfire smoke?

It is expected that the relative contributions of fire emissions to O<sub>3</sub> at a remote site such as GOTH will be higher than at a near-urban site like RFLAT [see Jaffe *et al.*, 2008], and these contributions may increase during high-fire summers or under the influences of long-range transport of smoke-related precursors and O<sub>3</sub>. A detailed assessment of the possible covariance of O<sub>3</sub> from wildfire smoke and the meteorological factors that contribute to high O<sub>3</sub> is beyond the scope of this study. It is, however, reasonable to assume that any confounding in the relationships between heights and O<sub>3</sub> is minimal in areas more strongly affected by large-scale sources of urban and industrial emissions.

We find that for the study domain, site R<sup>2</sup> (MDA8 O<sub>3</sub> versus 500 hPa heights) and elevation are well correlated. The regression between site R<sup>2</sup> and elevation for all 90 sites yielded a subsequent R<sup>2</sup> of 0.21. For sites not classified as rural, this subsequent R<sup>2</sup> increases to 0.53; in each case the null hypothesis is rejected ( $p=0.05$ ). The effects of 500 hPa heights on July MDA8 are therefore more pronounced at higher altitude sites, especially those that are urban or within close proximity to an urban area (elevation accounts for 53% of the site-to-site variation in response to 500 hPa heights for these sites). Plots of the two regressions described here are presented in the supporting information Figure S2.

#### 4. Analysis of the Relationships Between July MDA8 and Meteorological and Climate Variables Using NARR, GPCC v6, and NRCM-Chem

##### 4.1. Analysis of the Relationships Between July MDA8 and NARR Variables, GPCC v6, and Oceanic Niño Index for High and Low O<sub>3</sub> Years

It is clear from Figure 2 that July of 2002, 2003, 2006, and 2012 represent high periods for both O<sub>3</sub> and 500 hPa heights and that July of 1995, 1997, 2004, and 2009 represent low periods for both O<sub>3</sub> and 500 hPa heights, especially in Colorado. We use NARR data to explore mean 500 hPa heights for composites of the high and low periods. We also assess differences in mean MDA8, NARR surface scalar wind speeds, NARR PBL heights, and GPCC v6 precipitation anomalies. The results of these analyses are presented in Figure 3.

Figures 3a and 3b show the mean 500 hPa height contours for the high-O<sub>3</sub> and low-O<sub>3</sub> composites, respectively. For the high-O<sub>3</sub> cases, a mean Four Corners high with a 5940 m peak is present while for the low-O<sub>3</sub> cases, the high pressure is weaker (5920 m) and farther south with a center over southwest New Mexico. A map of terrain and key geographical features of the Four Corners region is presented in the supporting formation Figure S3. Ellis *et al.* [2000] found that for summer days with O<sub>3</sub> exceedances in and near Phoenix, Arizona, the composite 500 hPa analysis showed a 5935 m hPa high centered over the Four Corners, and their findings are similar to ours in the sense that the proximity of an upper level ridge was determined to be conducive to high O<sub>3</sub>. The differences between July MDA8 for the high and low O<sub>3</sub> cases for sites with available data for these years are also shown in Figure 3a. Mean July MDA8 O<sub>3</sub> decreases in portions of California and in Texas when the Four Corners high is stronger and over southern Colorado. The maximum decrease is 12 ppb at Azusa in the LA Basin. O<sub>3</sub> increases in this case over the Four Corners states and essentially under the core of the high. The highest increases are generally in the Colorado Front Range with as much as 13 ppb at RFLAT, NREL, and CRG.

Figure 3c shows the changes in scalar wind speeds between the two composites. Speeds are generally greater in the high-O<sub>3</sub>/heights case over the Great Plains but decrease by 1 to 3 m/s over the higher terrain

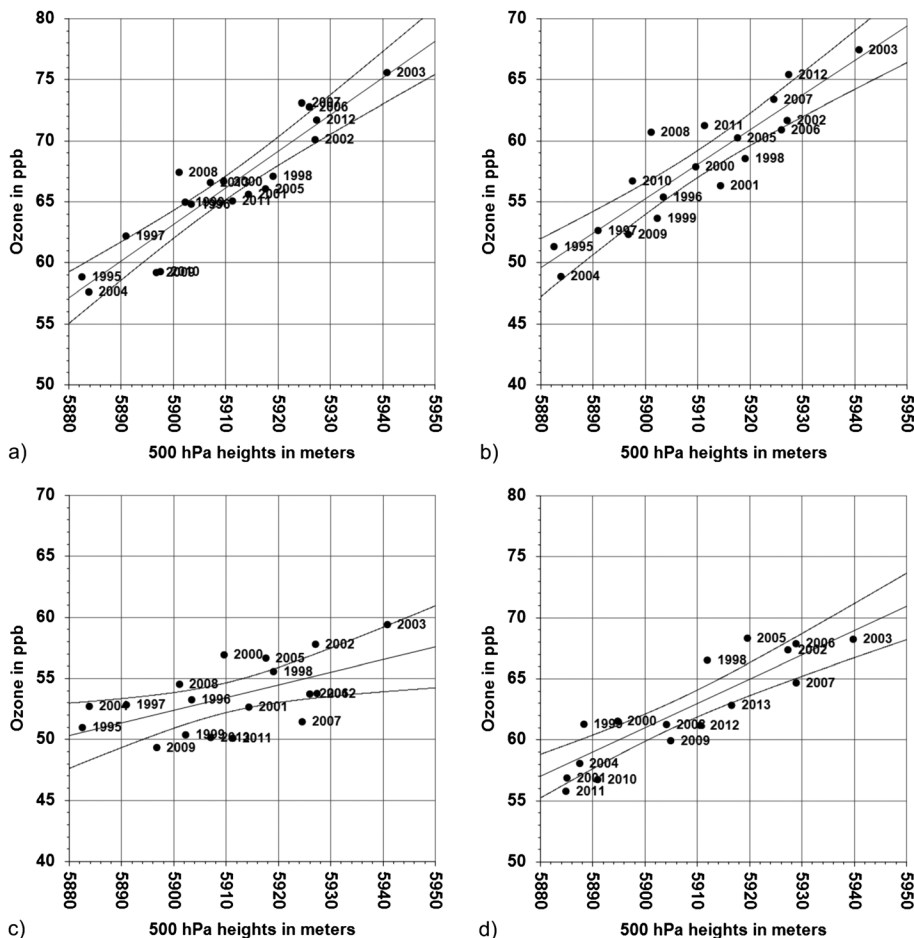
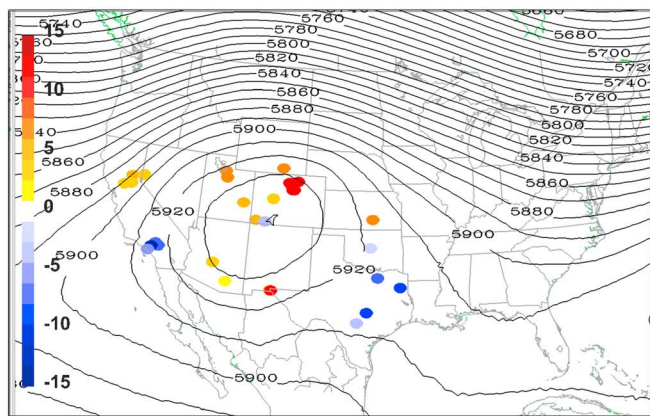


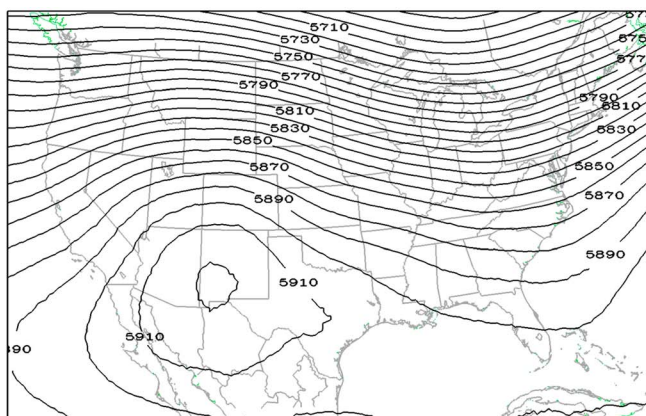
**Figure 2.** Linear regression with confidence limits between July Mean MDA8 O<sub>3</sub> and July mean NCEP/NCAR Reanalysis 500 hPa heights for (a) RFLAT northwest of Denver; (b) CRG near downtown Denver; (c) GOTH, a high-altitude site in west-central Colorado; and (d) SLCH in Salt Lake City, Utah; in each case the null hypothesis is rejected ( $p = 0.05$ ).

of Wyoming, Colorado, and Utah. PBL heights (Figure 3d) are generally 100 to 300 m larger over the Great Plains states, Wyoming, western Colorado, and much of the Colorado Plateau in the high-O<sub>3</sub>/heights case. Only minor positive or negative differences are observed along the northern and southern Colorado Front Range and in the vicinity of Salt Lake City, Utah. These regions are home to the Denver and Salt Lake City area monitors. Comparatively shallow mixing in these urban corridors can certainly lead to elevated local O<sub>3</sub>. In the case of the Front Range, for example, cooler air masses can affect the eastern plains of Colorado while a Four Corners ridge is in place, and this can result in shallower mixing over the plains and deep mixing over the mountains to the west. The presence of a strong Four Corners upper level high leads to lower wind speeds in much of the region's higher terrain, increased PBL heights in the higher terrain, and subsequent increases in regional O<sub>3</sub>.

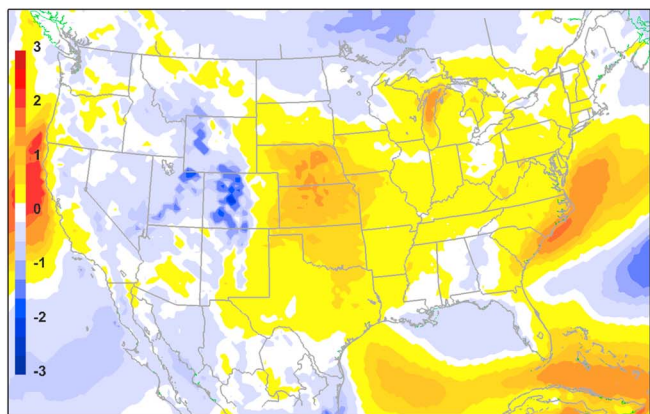
We also sought to understand the possible relationships between regional precipitation and soil moisture and O<sub>3</sub> during high and low 500 hPa height regimes. Figures 3e and 3f show July GPCC v6 precipitation anomalies with respect to the 1981–2010 climatology for the high- and low-O<sub>3</sub> and heights cases, respectively. The high-heights case shows a marked deficit in July precipitation (20 to 80 mm) over much of the Great Plains region, normal precipitation over the higher terrain areas of Colorado and the Colorado Plateau, and a slight increase over portions of Arizona and northwestern Mexico. The precipitation anomaly is small over the Colorado Plateau, Arizona, and New Mexico suggesting that the precipitation pattern is consistent with a normal southwest Monsoon in this region [Adams and Comrie, 1997]. For the low-heights case, the patterns of anomalies are generally reversed, with a reduced Four Corners region monsoon and increases in precipitation over much of the Great Plains and northern Rockies.



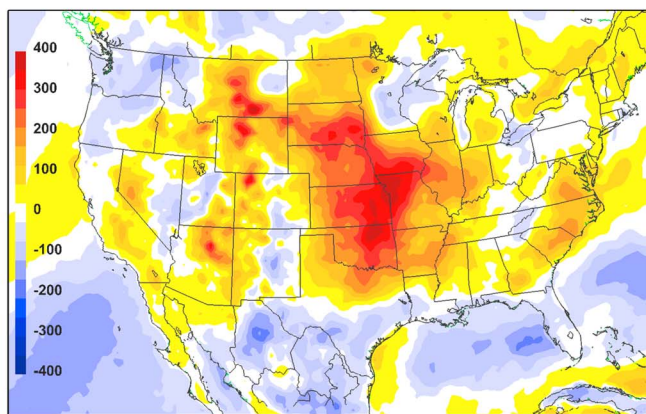
a) July NARR 500 hPa heights - 2002, 2003, 2006, and 2012



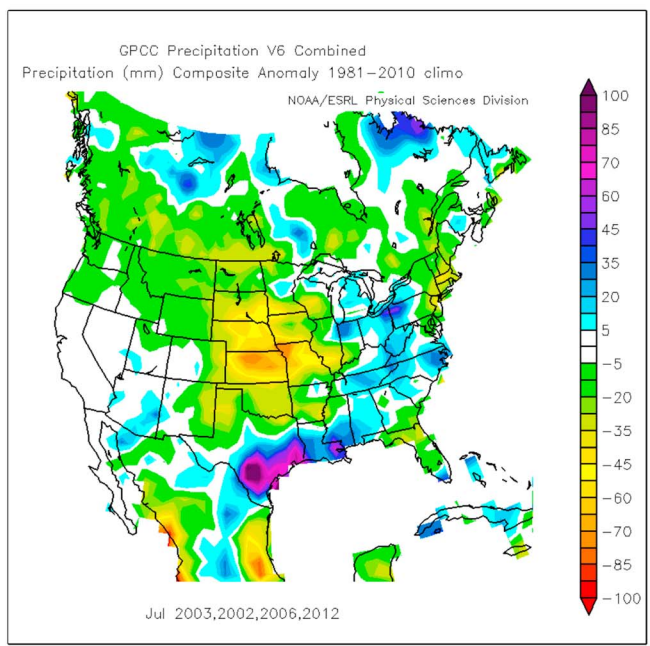
b) July NARR 500 hPa heights - 1995, 1997, 2004, and 2009



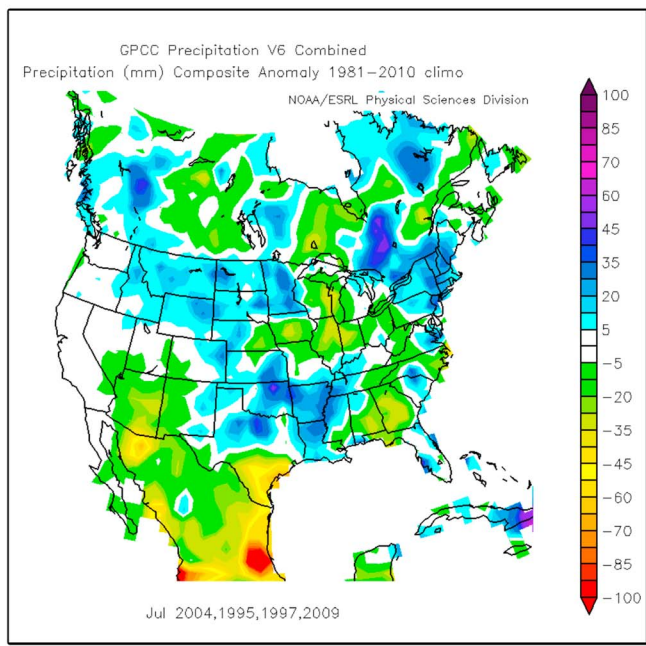
c) Differences in July NARR surface scalar wind speeds



d) Differences in July NARR PBL heights



e) Precipitation anomaly July 2002, 2003, 2006, and 2012



f) Precipitation anomaly July 1995, 1997, 2004, and 2009

**Figure 3.** Contours of July Mean NARR 500 hPa heights in meters for (a) 2002, 2003, 2006, and 2012 and (b) 1995, 1997, 2004, and 2009; differences in July mean NARR (c) surface scalar wind speeds in meters per second and (d) PBL height in meters (averages of 2002, 2003, 2006, and 2012 minus averages of 1995, 1997, 2004, and 2009); GPCC version 6 combined precipitation anomalies based on 1981–2010 climatology for July of (e) 2002, 2003, 2006, and 2012 and (f) 1995, 1997, 2004, and 2009; differences in mean July MDA8 O<sub>3</sub> in ppb for these two groups of years are also plotted in Figure 3a.

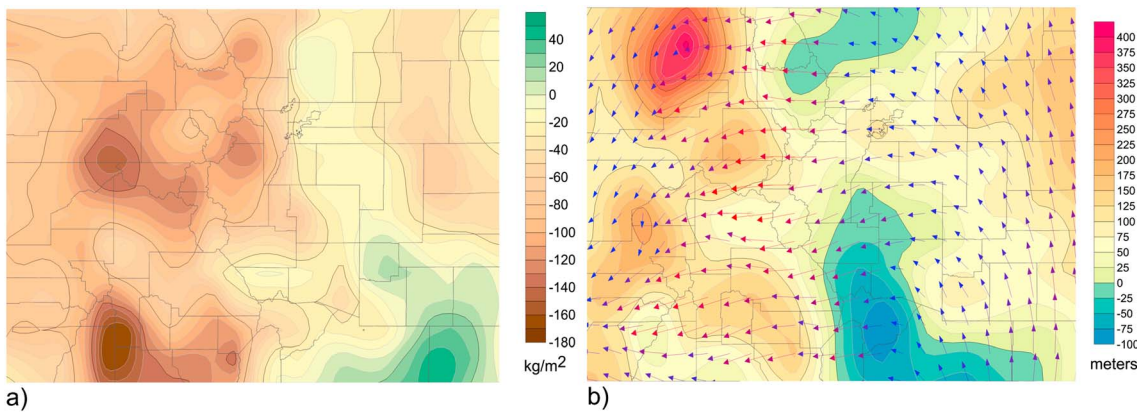


**Figure 4.** Differences in Colorado in (a) July mean NARR soil moisture in  $\text{kg}/\text{m}^2$  and (b) July mean NARR PBL height in meters and July NARR surface wind vector differences from Figure 6b (averages of 2002, 2003, 2006, and 2012 minus averages of 1995, 1997, 2004, and 2009).

We find that for the high- $\text{O}_3$ /heights regime, July NARR soil moisture levels are anomalously low over the higher terrain of western Colorado. Figure 4a shows that relative to the low  $\text{O}_3$ /heights regime, there is a soil moisture deficit of 50 to 180  $\text{kg}/\text{m}^2$  (50–180 mm) in the western, higher-terrain portion of Colorado. Figure 4b shows that for the high  $\text{O}_3$  and heights scenario, July monthly mean PBL heights are 50 to 400 m higher over this same portion of the state, while PBL heights in the center of the state are near normal. The juxtaposition of low soil moistures and deeper mixing over the mountainous western part of Colorado and near-normal soil moistures and mixing heights along the Front Range is consistent with an enhanced mountain-plains circulation and the resulting westward vector difference in surface winds shown in Figure 4b. The shift toward increased surface easterlies or reduced westerlies shown in Figure 4b is consistent with a relaxation of normal synoptic-scale forcing which could inhibit mountain-plains solenoid circulations.

*Bossert and Cotton [1994a, 1994b], Bossert et al. [1989], and Toth and Johnson [1985]* have described summer-time mountain-valley and terrain-induced mesocirculations along Colorado's Front Range from the plains westward across the continental Divide. These flows and circulations play an important role in the transport and distribution of  $\text{O}_3$  and its precursors in northeastern and north-central Colorado. *Bossert and Cotton [1994a]* have shown that reduced soil moisture in the mountains combined with the absence of significant synoptic-scale flows aloft can lead to enhanced mountain-plains solenoid circulations during the day and subsequent westward propagating density currents at night. Under clear skies, nighttime drainage flows can carry Denver and Front Range air pollutants northward and eastward along the Platte Valley. Daytime thermally driven upslope reverses these flows, carrying air pollutants toward the west and into higher terrain. At the same time, solenoid circulations that form with weak westerlies aloft can cause eastward or return flow at the top of a deep, daytime, mixed layer and sinking motion over the plains providing a mechanism for the potential return of air pollutants to the urban corridor. Nighttime subsidence over the higher peaks, ridges, and slopes replaces air entrained into slope and drainage flows, and this can introduce  $\text{O}_3$  and precursors from residual layers aloft into near-surface flows returning to the plains. In addition, the westward propagating density currents carry air pollutants to the west and north of the Continental Divide. Weak westerlies can bring this material back to the plains in subsequent periods. An increase in mixing heights over the higher terrain and lower soil moisture in this terrain indicates that the potential for enhancement in the solenoid and density current circulations is high during the high- $\text{O}_3$ /heights periods. When these are active, mountain-valley circulations are major factors in transport and dispersion and can lead to enhanced day-to-day local and regional accumulation of  $\text{O}_3$  and its precursors.

RFLAT west of Denver is representative of many of the sites in Colorado and Utah with high correlations with 500 hPa heights. Figures 5a and 5b show the distribution of RFLAT July MDA8 correlation coefficients by U.S. Climate Divisions in relation to the July Palmer Drought Severity Index (PDSI) and precipitation, respectively. These correlations were generated using the online U.S. Climate Divisions Data Set Seasonal Correlation tool provided by NOAA Office of Oceanic and Atmospheric Research/Earth System Research Laboratory Physical Sciences Division (NOAA/OAR/ESRL PSD) in Boulder, Colorado. For the entire study period (1995–2013), we find that RFLAT July MDA8  $\text{O}_3$  is moderately to significantly anticorrelated (correlation coefficients of  $-0.3$

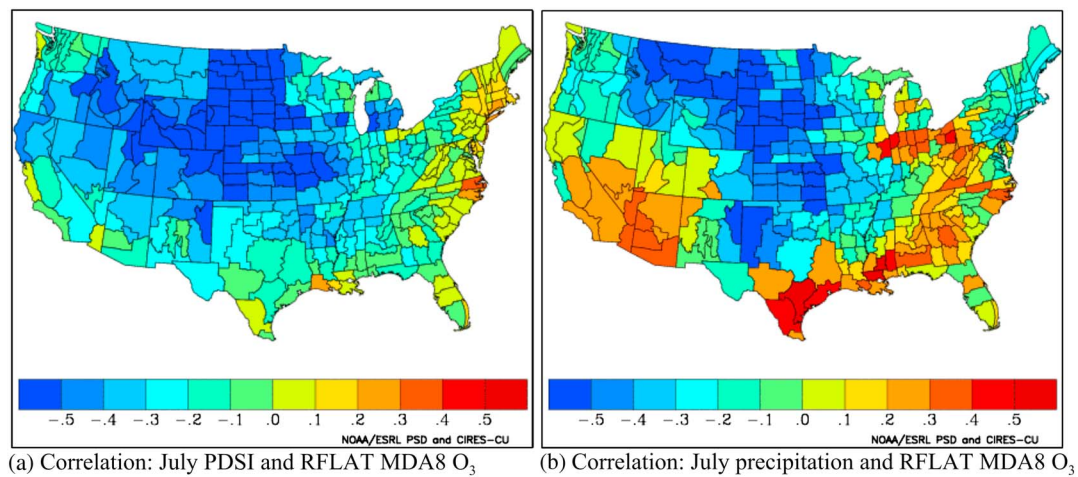


**Figure 5.** Correlations between RFLAT July MDA8 O<sub>3</sub> and U.S. Climate Divisions July (a) PDSI and (b) precipitation for 1995 through 2013.

to  $-0.6$ ) with the PDSI over eastern Colorado, Wyoming, Utah, and much of the Great Plains and Rocky Mountain region. In other words, high O<sub>3</sub> at this site is moderately to strongly correlated with increased drought conditions in these areas. Correlations in Figure 5b also show that elevated O<sub>3</sub> at RFLAT is slightly correlated with precipitation over western Colorado and moderately correlated (correlation coefficients of 0.2 to 0.4) with precipitation over Arizona, much of Utah outside of the Salt Lake City area, northwest New Mexico, and large areas of Nevada and California. These results may appear to be in conflict with the lower western Colorado soil moistures observed in the high-O<sub>3</sub>/heights years, but it is possible that a normal or enhanced monsoon occurs after a period of relative drought and that western Colorado represents a transition zone for a more significant monsoon centered in Arizona. Analysis of precipitation, soil moisture, and PDSI data for high- and low-O<sub>3</sub>/500 hPa heights regimes and the correlations between RFLAT O<sub>3</sub> and PDSI and precipitation show that we also need to consider the potential influences of Four Corners area thunderstorms on Colorado and Utah July MDA8. These are the states where the association between 500 hPa heights and MDA8 is generally the strongest.

Lightning NO<sub>x</sub> [Cooper *et al.*, 2007] and mesoscale stratospheric intrusions of O<sub>3</sub> from thunderstorms [Pan *et al.*, 2014] can lead to free tropospheric enhancements of O<sub>3</sub> during the North American summer. Using the GEOS-Chem chemical transport model, Zhang *et al.* [2014a] determined that lightning accounted for an increase in mean June-August MDA8 of 6 to 10 ppb in Utah, Colorado, Arizona, and New Mexico in 2007. Based on the data in Figure 2, July 2007 had relatively high O<sub>3</sub> at the two Front Range sites and SLCH but a low O<sub>3</sub> at GOTH. We can infer from Figures 3 and 5 that the enhanced Four Corners 500 hPa high present during high O<sub>3</sub> years is associated with monsoon precipitation on its southern and western sides, which may explain the weaker response of MDA8 in these areas evident in Figures 1 and 3a. The weak upper level flow in the center of the high is in a position to circulate lightning NO<sub>x</sub> and/or stratospheric O<sub>3</sub> from storm-related stratosphere to troposphere exchange throughout the Four Corners states, including areas of Utah and Colorado that may have below-normal convective activity and lower cloud cover. It is in the center of this high that increases in O<sub>3</sub> during high O<sub>3</sub> years are at their peak.

Using July NLDN total lightning strike count data from the National Climatic Data Center (<https://www.ncdc.noaa.gov/data-access/severe-weather/lightning-products-and-services>) as an indicator for thunderstorm activity, we find that lightning strikes generally decrease across portions of northern Utah and Colorado and the High Plains, including the eastern plains of both Colorado and New Mexico during the high-O<sub>3</sub>/heights years while lightning strikes increase over much of Arizona, southern Utah, the mountains of central and southwestern Colorado, and western New Mexico (see supporting information Figure S4). These patterns are consistent with the precipitation anomalies for high- and low-O<sub>3</sub>/heights years presented in Figures 3e and 3f. Because of the increases in thunderstorm activity over large areas within the mean Four Corners upper level ridge during high-O<sub>3</sub>/heights years, we cannot rule out the possibility that thunderstorm-related

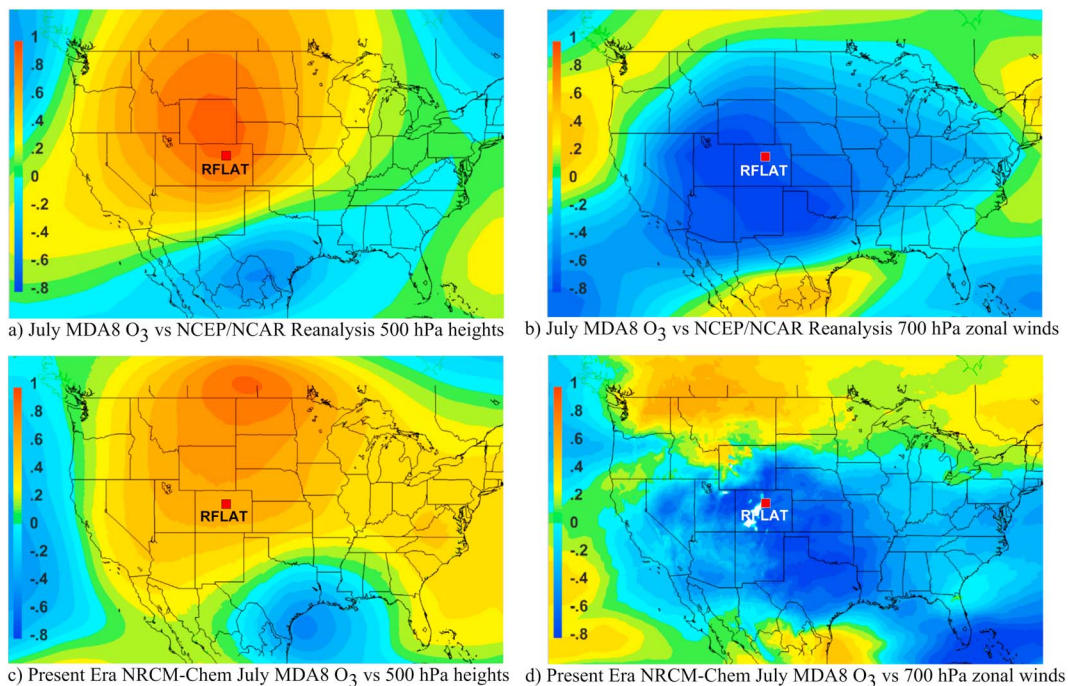


**Figure 6.** Pearson correlations for RFLAT July mean MDA8  $O_3$  and (a) NCEP/NCAR Reanalysis 500 hPa heights and (b) 700 hPa zonal winds for 1995–2013; and correlations for RFLAT July mean MDA8 and (c) 500 hPa heights and (d) 700 hPa zonal winds based on the Present Era NRCM-Chem model runs and the CCSM 3.0 climate model.

$O_3$  explains some of the variance in the relationship between  $O_3$  and 500 hPa heights, especially in Colorado and Utah. Demonstrating or quantifying the role of storm-related  $O_3$  here is not part of our study.

We also explore correlations between the June–July–August ONI (an ENSO index based on the 3 month running average sea surface temperature anomaly for the area within 5°N and 5°S and 120°W and 170°W) and  $O_3$  in Colorado and Utah. Correlations between the ONI and the 9 Wasatch Front sites in Utah and the 14 Front Range sites in Colorado were highly variable, ranging from –0.51 to 0.28 with means of –0.11 for Utah and –0.17 for Colorado. For the high- $O_3$ /heights years the mean ONI was 0.3 representing neutral conditions, and for the low- $O_3$ /heights years the mean ONI was 0.6 representing weak El Niño conditions. We conclude that the connections between midsummer ONI and July MDA8 in these states are generally weak, with a weak tendency for lower  $O_3$  during El Niño summers.

#### 4.2. Testing the Relationships Between $O_3$ and Meteorology Using NRCM-Chem

We investigate the occurrence of similar relationships between meteorology and  $O_3$  in the NRCM-Chem. First, we examine Pearson correlations between measured RFLAT July MDA8 and NCEP/NCAR Reanalysis 500 hPa heights and 700 hPa zonal winds across the U.S. using a tool provided by NOAA/OAR/ESRL PSD in Boulder, Colorado. The results for 500 hPa heights and 700 hPa zonal winds are presented in Figures 6a and 6b, respectively. These show that observed RFLAT MDA8 is strongly correlated with heights in the northern Rocky Mountain states, with the peak effect centered on Wyoming and Colorado, and that RFLAT MDA8 is strongly anticorrelated with 700 hPa zonal winds throughout much of the central and western portions of the U.S., with the peak effect over the Four Corners states and northern Texas. Similar patterns of correlations are found for July MDA8  $O_3$  from the NRCM-Chem Present Era simulation for a location equivalent to RFLAT (Figures 6c and 6d). In the NRCM-Chem Present Era model, the peak response to 500 hPa shifts northward to the border between Canada and the U.S., which is likely caused by the model not fully representing the complex topography and dynamics of this region with a 12 km grid resolution. The large area of anticorrelation with 700 hPa zonal winds is comparable with the results in Figure 6b.

We also calculated the correlations between July MDA8 and 500 hPa using the NRCM-Chem Present Era, Future, and Future A model runs for locations representative of RFLAT and SLCH. Future era results were

considered because they provide a means to test the influence of local sources and terrain on O<sub>3</sub>. We tested the sensitivity of the model correlations to the way surface sites are selected by calculating mean MDA8 within 0.1, 0.2, 0.3, 0.5, and 1.0° grids and the maximum within a 1.0° grid centered on the coordinates for the two monitoring sites. The results for these methods were similar, and the values for means within a 0.1° grid were used in this analysis.

Pearson correlations for MDA8 and NCEP/NCAR 500 hPa heights at RFLAT and SLCH are 0.92 and 0.89, respectively (Table 1). The NRCM-Chem Present Era reproduces this pattern, and for RFLAT and SLCH MDA8 exhibits weaker but robust responses with correlations of 0.67 and 0.64, respectively. In the NRCM-Chem Future scenario, emissions of O<sub>3</sub> precursors over the U.S. are greatly reduced compared with the Present Era case, with NO emissions reduced by 57% and non-methane volatile organic compounds (NMVOC) emissions reduced by 69% [Pfister *et al.*, 2014]. In this scenario the correlation for RFLAT drops to 0.33 and the correlation for SLCH drops to near zero. In the Future A case, where emissions were kept at Present Era levels and only global climate and inflow changed (including an increase in background O<sub>3</sub> as a result of increased global methane levels), the correlation for RFLAT increases to 0.82 and the value for SLCH drops to 0.38. The latter might be explained by the relatively larger role of background O<sub>3</sub> in the Future A scenario.

Except in the case of greatly reduced precursor emissions, the NRCM-Chem model runs reproduce a robust relationship between MDA8 and 500 hPa at these two high-altitude sites. The fact that the NRCM-Chem captures this effect and yields much lower correlations at RFLAT and SLCH when emissions are greatly reduced suggests that elevated 500 hPa heights lead to enhanced O<sub>3</sub> production and accumulation and that these increases in O<sub>3</sub> are associated with local or subregional emissions and favorable meteorology in elevated terrain.

This conclusion is also supported by looking at differences in July monthly mean NARR winds between the 4 high-O<sub>3</sub>/heights and 4 low-O<sub>3</sub>/heights years (described earlier) for the 500 hPa and surface levels, respectively, over Colorado (Figures 7a and 7b). During the four summers with elevated O<sub>3</sub>/heights, there is a pronounced increase in easterlies and/or reduction in westerlies at both altitude levels. The differences in surface winds are highest over the high terrain areas of western Colorado where data from Figure 4 show that NARR soil moistures are lower and mixing heights are higher during these 4 years. Figures 7c and 7d show the differences in July monthly mean NRCM-Chem Present Era winds between the upper and lower 20 percentile RFLAT MDA8 for 500 hPa and the surface, respectively. As in Figures 7a and 7b, the Present Era wind differences between high- and low-O<sub>3</sub> cases show a marked increase in easterlies or reduction in westerlies over the higher terrain of western Colorado. In both the historical and modeled cases, these differences provide evidence that conditions favorable to mountain-valley circulations are present during years with higher O<sub>3</sub>.

The changes in surface winds shown in Figures 7b and 7d suggest an increase in southerly and southeasterly flows on the eastern plains of Colorado during high O<sub>3</sub> periods. Southerly and southeasterly surface flows are associated with the Denver Cyclone, a cyclonic gyre that forms to the north of the Palmer Divide south and southeast of Denver. This mesoscale circulation can be associated with high stability in surface layers [Szoke, 1991] or an elevated layer of stability in the PBL [Szoke and Augustine, 1990; E. J. Szoke, personal communication, 1994]. Through operational forecasting of air quality in eastern Colorado, we have observed that the Denver Cyclone is more pronounced when there is a layer of high stability or a cap above the surface mixed layer and below the 700 hPa level. The Denver Cyclone circulation also leads to upslope flow along the Platte Valley toward Denver and can contribute significantly to poor air quality [Reddy *et al.*, 1995]. Because it can form when upslope flow along the plains does not reach above 700 hPa and this flow is decoupled from flows in the higher terrain to the west, it may not be associated with deep westward transport. It does, however, represent another potential terrain-related mechanism for limiting area-wide dispersion of O<sub>3</sub> and its precursors when 500 hPa heights are high.

## 5. The Role of Terrain-Driven Circulations Under Persistent 500 hPa High-Pressure Systems

Analysis of transport patterns and historical MDA8 data for Colorado's Front Range points to the role of thermally driven upslope flows during the summer months. In Figure 8, we present the relative density of

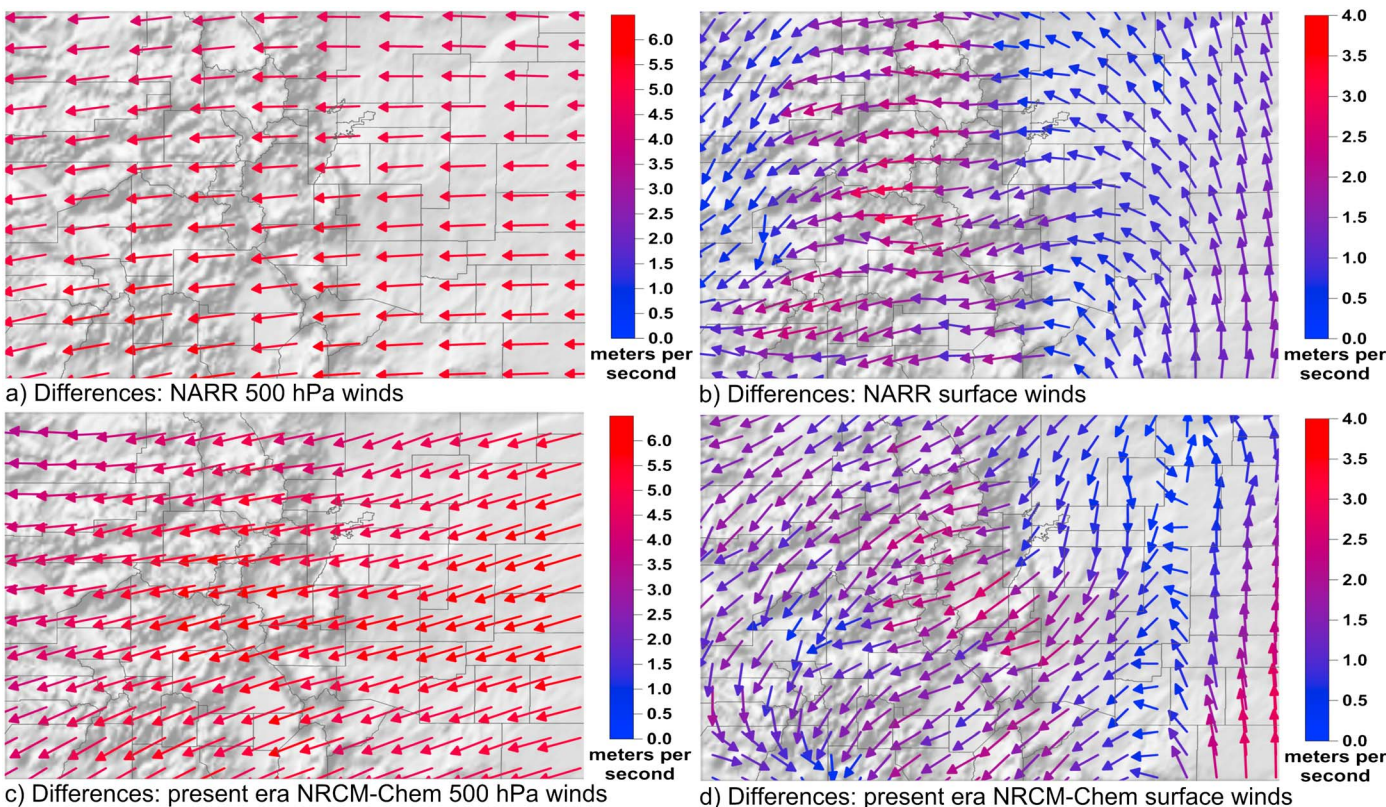


**Figure 7.** Differences in Colorado July monthly mean winds in m/s for (a) NARR 500 hPa and (b) NARR surface levels (averages of 2002, 2003, 2006, and 2012 minus averages of 1995, 1997, 2004, and 2009); differences in NRCM-Chem Present Era winds for the upper and lower 20 percentile July RFLAT MDA8 cases for (c) 500 hPa and (d) surface levels—vector spacing does not reflect native grid resolutions.

NOAA HYbrid Single-Particle Lagrangian Integrated Trajectory (HYSPLIT) [Draxler and Rolph, 2014; Rolph, 2014] 24 h back trajectory points for each hour in each 8 h period for the four highest MDA8 O<sub>3</sub> concentrations each year at FTCW, RFLAT, and CHAT for 2006 through 2008, assuming 100 m arrival heights and using EDAS 40 km meteorological fields.

This plot shows that daytime transport on high-O<sub>3</sub> days moves air from the wider areas of the Platte Valley (extending from Denver to Greeley (GRE)) upvalley and in the direction of the foothills and higher terrain. This pattern of transport is consistent with typical daytime thermally driven upslope flow toward the Divide as influenced by local drainages and described by Toth and Johnson [1985]. In addition, the flow originates in the wider Platte Valley where down-valley nighttime and morning drainage flows move emissions from Denver and the surrounding urban areas.

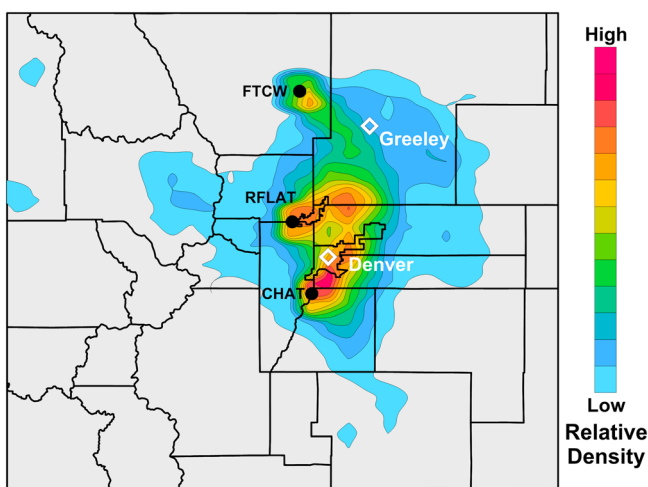


**Figure 8.** Relative density of NOAA HYSPLIT 24 h back trajectory points for each hour in each 8 h period for the four highest MDA8 O<sub>3</sub> concentrations each year at FTCW, RFLAT, and CHAT for 2006 through 2008 assuming 100 m arrival heights and using EDAS 40 km meteorological fields—lowest densities are not shown.

Thermally driven upslope flows along the Front Range transport O<sub>3</sub> and its precursors westward beyond these three monitoring sites toward and in some cases beyond the Continental Divide.

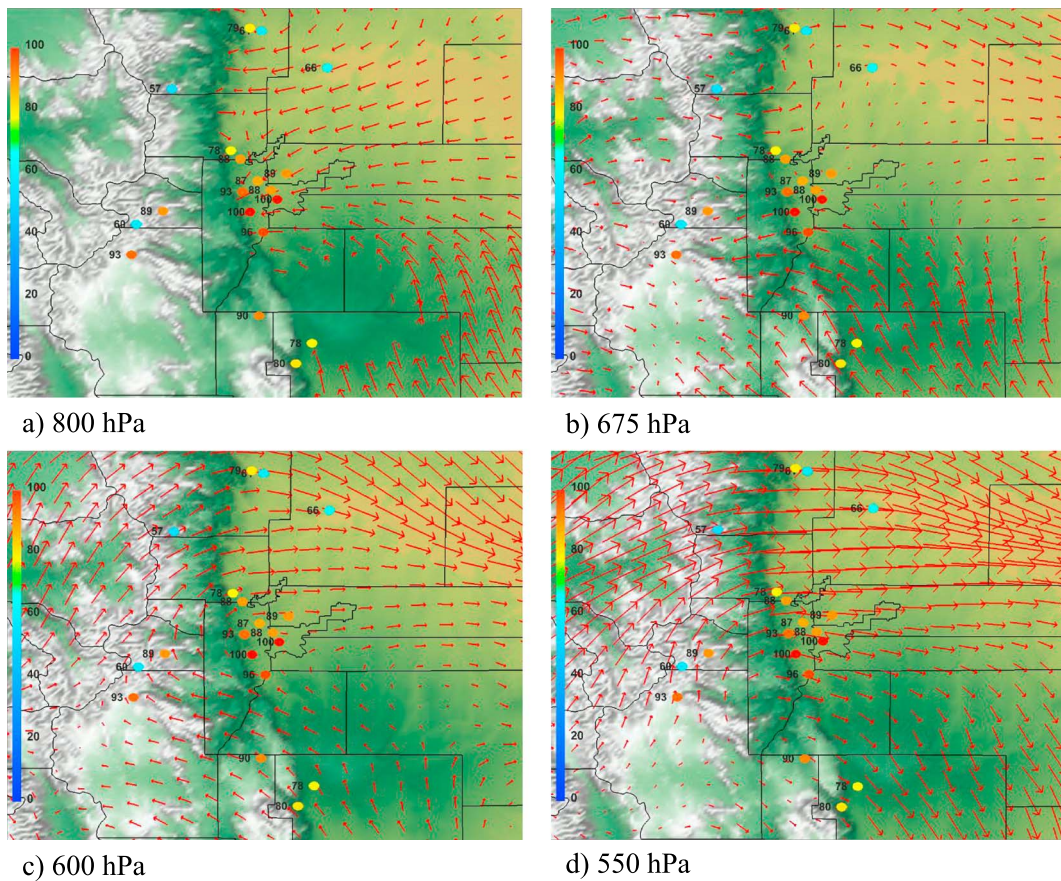


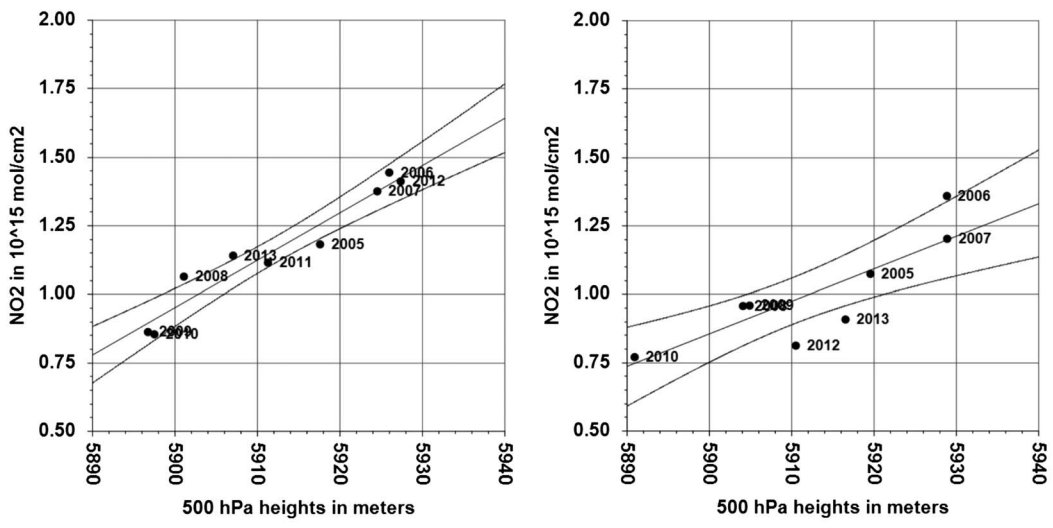
**Figure 9.** One hour O<sub>3</sub> for select Colorado sites for 19 MST 10 July 2008 with NCEP NAM12 17 MST analysis run winds for (a) 800 hPa, (b) 675 hPa, (c) 600 hPa, and (d) 550 hPa. Maps show mountain-plains solenoid circulation and its impacts on O<sub>3</sub>. NAM12 mixing heights for 17 MST were near the 475 hPa level (approximately 6 km msl) over NREL and Kenosha Pass (KEN).

We now consider the westward extent of transport and the potential role of the mountain-plains solenoid circulation in the region during the high- $O_3$  event of 10 July 2008.

Ozonesonde profile data at 12:15 MST on 10 July 2008 (not shown here) obtained from the National Oceanic and Atmospheric Administration (NOAA) Global Monitoring Division for a sonde launched near Boulder, Colorado (roughly 31 km northwest of Denver), indicate that midday O<sub>3</sub> concentrations ranged from 88 to 97 ppb in the layer below 3 km mean sea level (msl), gradually dropping to 70 ppb at 6 km msl. Based on the potential temperature profile, we can say that the top of the PBL was just above the 6 km level. Potential temperatures in the PBL varied only between 322° and 323°K from just above the superadiabatic layer near the ground to 6.1 km or 485 hPa.

In the supporting information Figure S5a, a plot of data from the NCEP NAM12 analysis run for 11 MST shows that a 5810 m 500 hPa ridge was centered over the Four Corners region, and the supporting information Figure S5b shows the locations of the O<sub>3</sub> monitoring sites and the topography of the area. In addition to monitor sites already listed in Table 1, this analysis includes U.S. Forest Service 2B Tech monitor sites as described by *Musselman and Korfmacher* [2014]. These are MEV, KEN, MTEV, and MTG sites at 2360, 3098, 4300, and 3518 m msl, respectively. The Front Range sites FTCW, WLBY, and GRE are at 1571, 1554, and 1484 m msl, respectively (Table 2).

A well-developed mountain-plains circulation was in place in this area during the afternoon of 10 July 2008. One hour O<sub>3</sub> concentrations at 19 MST are shown in each map in Figure 9 together with NAM12 analysis run winds for 17 MST for the (a) 800 hPa, (b) 675 hPa, (c) 600 hPa, and (d) 550 hPa levels. At 19 MST, mountain sites recorded concentrations of ~90 ppb. Concentrations of 87 to 100 ppb were measured in the immediate Denver area. Low-level thermally driven upslope flow is apparent across the plains and valley locations



a) Denver NCEP/NCAR Reanalysis grid      b) Salt Lake City NCEP/NCAR Reanalysis grid

**Figure 10.** Linear regressions between (a) Denver-area and (b) Salt Lake City-area NCEP/NCAR Reanalysis grid mean July level 3 OMI tropospheric NO<sub>2</sub> (2005 through 2013) and July mean NCEP/NCAR Reanalysis 500 hPa heights with confidence limits.

and continues through the 600 hPa level over the southern part of the area depicted in Figure 9. Flows from near the surface through 600 hPa would have been able to carry O<sub>3</sub> and its precursors from urban plains locations (Denver and Colorado Springs) to the mountains. Westerly flow at 550 hPa, which was below the top of the PBL at this time (485 hPa from the Boulder ozonesonde), would have allowed return flow of O<sub>3</sub> and its precursors within the top of the mixed layer over the Denver and Colorado Springs areas where the highest surface concentrations on the plains occurred. In the northern portion of this area, the solenoid circulation was probably shallower and farther east of the highest terrain. Here westerly flow was apparent over much of the area above 675 hPa and was much stronger aloft than in the southern portions of the area. Likely as a result of a greater occurrence and strength of westerlies in the mixed layer, surface O<sub>3</sub> at northern sites ranged only from 57 to 79 ppb.

The mountain-plains solenoid has the capability to limit horizontal transport away from source areas and reintroduce O<sub>3</sub> and its precursors to areas nearby via return flow aloft within the PBL and downward motion over the plains. In the absence of deep upslope flow, however, shear associated with westerlies in the mixed layer can more effectively disperse air pollutants in the column. It is one of our hypotheses that the response of July MDA8 to 500 hPa heights is particularly strong along Colorado's Front Range because mountain-valley circulations are more prominent and well developed with increasing 500 hPa heights. In addition, we hypothesize that the daytime westward return of nighttime and early morning emissions that have accumulated in near-surface layers in the wider Platte Valley also enhances July MDA8 when upper level high-pressure systems are strong.

## 6. Using 500 hPa Heights to Correct Trends in July MDA8 and OMI Tropospheric NO<sub>2</sub>

### 6.1. Relationships Among July 500 hPa Heights, OMI Tropospheric NO<sub>2</sub>, and MDA8

Here we describe additional statistical analyses of July OMI NO<sub>2</sub>, 500 hPa heights, and MDA8 for the Front Range region of Colorado and the Wasatch Front region of Utah that provide further evidence for the effects of local circulations on O<sub>3</sub> and NO<sub>2</sub> when 500 hPa heights are elevated. We calculated July mean OMI tropospheric NO<sub>2</sub> for the 2.5° by 2.5° NCEP/NCAR Reanalysis grid cells that include Denver (supporting information Figure S1) and Salt Lake City (grid cell not shown here). The Denver grid cell covers much of the terrain tied to local circulations and includes the urban corridor, the Platte Valley to the north of Denver, the foothills, and the Continental Divide. Linear regressions between OMI July mean tropospheric NO<sub>2</sub> and 500 hPa heights for these two grid cells are shown in Figure 10 and are robust with  $R^2$  values of 0.93 for the Front Range and 0.77

for the Wasatch Front (in each case the null hypothesis is rejected,  $p = 0.05$ ). Front Range NO<sub>2</sub> increases nearly linearly with heights. This is consistent with the expected effects of local circulations on accumulation of NO<sub>2</sub> and the increase in the number of days with high NO<sub>2</sub> when monthly mean heights are high—as opposed to changes in photochemistry that would likely be nonlinear. In addition, correlations between OMI NO<sub>2</sub> and July MDA8 O<sub>3</sub> at three sites in Colorado—RFLAT, NREL, and FTCW—are 0.97, 0.93, and 0.93, respectively. Correlations between OMI NO<sub>2</sub> and July MDA8 O<sub>3</sub> at three sites in Utah—SLCH, NPROV, and LOG—are 0.86, 0.76, and 0.78, respectively. These results confirm that NO<sub>2</sub> increases with increasing heights and that local O<sub>3</sub> is strongly associated with the presence of local NO<sub>2</sub>.

## 6.2. Trends in July MDA8 and OMI Tropospheric NO<sub>2</sub> Corrected for the Effects Meteorology

Robust linear regressions with heights for July MDA8 and OMI tropospheric NO<sub>2</sub> at many sites in the western U.S. can be used to correct and assess trends in July MDA8, effectively accounting for much of the variance associated with meteorology and climatology and yielding time series that are more directly related to trends in precursor emissions, background, transboundary O<sub>3</sub>, and other factors. Figure 11a shows the 1995–2013 time series for July MDA8 for 14 Front Range area monitors fitted with a LOESS curve [Cleveland, 1979] based on a relatively low smoothing parameter of 0.15, which makes the curve more responsive to year-to-year variability. The use of larger values for the smoothing parameter would lead to more gradual changes from year to year. Figure 11b shows the same analysis for nine Utah Wasatch Front sites in and around the greater Salt Lake City region. Large drops in MDA8 are apparent in 2004 and 2009. For the Front Range, a significant long-term increase in MDA8 extends from 1995 to 2003. In Figures 11c and 11d we have fit the same LOESS curves to weather-corrected data for the Front Range and Wasatch Front sites. Here the data points are the sums of the monitoring site sampling-period means and residuals of the regressions between July MDA8 and local grid cell 500 hPa heights.

After correcting for the effects of meteorology, for the Front Range we see a stable time series for 1995 through about 2004 (a period with steadily increasing 500 hPa heights through 2003), an increase of roughly 5 ppb through 2008, a sharp drop of about 7 ppb by 2009, and an increase of roughly 5 ppb from 2009 to 2013. The 2009 drop is likely associated with the effects of the economic recession in 2008. The effects of the recession on NO<sub>2</sub> have been well documented [Russell *et al.*, 2012; Tong *et al.*, 2015]. The year 2009 was also low for 500 hPa heights, and the correction for heights makes a more accurate comparison between 2009 and pre-recession years possible. Both the more or less steady increase in corrected MDA8 after 2004 and from 2009 through 2013 could be the result of concurrent increases in local oil and gas production and/or growth in emissions from other local sources (the estimated population of the Northern Front Range region increased from 4.61 to 5.27 million from 2004 to 2013 [Colorado Department of Local Affairs, 2015]).

Not only is the Platte Valley a location for pooling of NO<sub>2</sub> and other pollutants under drainage flow across the urban corridor, it has a high density of oil and gas production facilities that emit VOCs and NO<sub>x</sub>. In the supporting information Figure S1 of their paper, Pétron *et al.* [2014] showed that oil production in Weld County increased from less than 1 million bbls/month in 2004 to roughly 3.5 million bbls/month by mid-2012. In the same period, the numbers of oil and gas wells in Weld County nearly doubled. In 2012, Weld County accounted for 74% of the oil produced in Colorado. Emissions of O<sub>3</sub> precursors from oil and gas activities along the Platte Valley almost certainly contribute to O<sub>3</sub> formation in the region. The nature of terrain-mediated flows and evidence from satellite NO<sub>2</sub> and HYSPLIT analyses spanning years prior to the steep increases in oil and gas production, however, support the conclusion that the Platte Valley from Denver northward is a source region for urban-region O<sub>3</sub> precursors in general, not just those from oil and gas sources. Quantifying the effects of oil and gas emissions on the corrected O<sub>3</sub> trend is beyond the scope of this study, but the trend may lend support to work designed to explore these interrelationships.

The corrected trend for the nine Wasatch Front sites tells a different story. Local peaks in MDA8 occur in 2000, 2005, and 2008. The postrecession period is associated with a drop of roughly 5 ppb. Unlike the Front Range, the Wasatch Front has experienced a general decline of roughly 6 ppb since 2000. The cause of this decline is not explored here, but it is worth noting that most of Utah's oil and gas development in recent years has been in eastern Utah on the other side of high mountains to the east of the Wasatch Front urban corridor.

Trends in raw and weather-corrected July OMI tropospheric NO<sub>2</sub> (the sum of the period mean and the residuals of the regressions with 500 hPa heights) for 2005–2013 are presented for the Front Range in

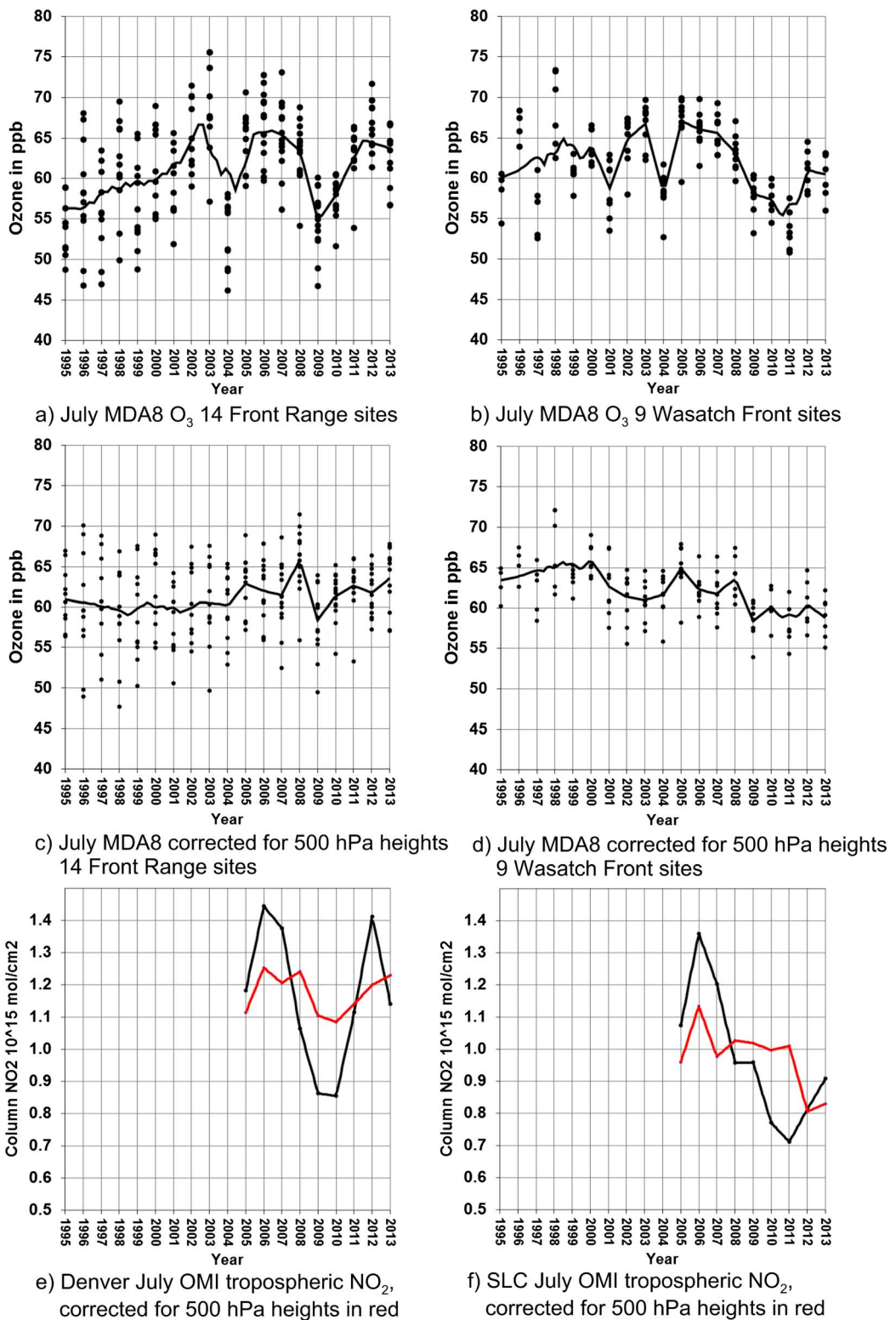


**Figure 11.** July mean trends in MDA8  $O_3$  for (a) 14 Colorado Front Range sites including Colorado Springs, Denver, Boulder, Fort Collins, Greeley, and nearby foothills and mountains east of the Continental Divide and (b) 9 Utah Wasatch Front sites including Salt Lake City, Brigham City, Logan, and Bountiful; July mean trends after correction for NCEP/NCAR Reanalysis 500 hPa heights for (c) the same 14 Colorado Front Range sites and (d) the same 9 Utah Wasatch Front sites; and trends in area-averaged July mean level 3 OMI tropospheric  $NO_2$  before and after correction for NCEP/NCAR Reanalysis 500 hPa heights for (e) the Denver and (f) the Salt Lake City NCEP/NCAR Reanalysis grid cells.

Figure 11e and the Wasatch Front in Figure 11f. Figure 11e shows a high period in weather-corrected NO<sub>2</sub> from 2006 to 2008, a drop in 2009, and a subsequent gradual increase from 2010 to 2013. Figure 11f shows a more substantial and persistent decline during the entire period, which is consistent with the trend in weather-corrected O<sub>3</sub> for the Wasatch Front.

Cooper *et al.* [2012] have examined 1990–2010 trends in O<sub>3</sub> for rural sites and noted that despite significant reductions in precursor emissions, only 17% of western rural U.S. sites had significant reductions in the 95 percentile concentrations during the period. Although the authors considered the changes in O<sub>3</sub> in relation to regional temperature trends, their results may not reflect the substantial influence of persistent upper level high pressure on peak summer O<sub>3</sub> concentrations demonstrated here and the confounding effects of trends in 500 hPa heights. In addition to inflow of higher background and other factors that may explain the trends that they observed, the impacts of meteorology during peak O<sub>3</sub> season can be substantial. Our approach offers a potentially powerful method for correcting trends in satellite-derived NO<sub>2</sub> and peak O<sub>3</sub> for tracking and assessing changes in standard-relevant concentrations of MDA8.

In this regard, this method could be of particular value to state, local, and federal air quality managers who are tasked with assessing the effectiveness of control strategies over time and the impacts of sources beyond their jurisdiction. State and local air quality management agencies are often called upon to assess O<sub>3</sub> trends in a weight of evidence analyses in support of a State Implementation Plan for O<sub>3</sub>. NCEP/NCAR Reanalysis data for 500 hPa heights (and other variables described in this paper), and MDA8 data are readily and freely available online. Regressing mean MDA8 and meteorological variables and fitting an appropriate smoothing curve to the sums of the residuals and site means are straightforward tasks that can be completed with a minimum of resources. Our method also offers an alternative to the use of Kolmogorov-Zurbenko filters described by Eskridge *et al.* [1997], Milanchus *et al.* [1998], and Porter *et al.* [2001] which have in the past been applied by the Colorado Department of Public Health and Environment and other agencies to O<sub>3</sub> time series, after the application of a correction for surface temperature. The advantage of our method is that it identifies patterns and signals specific to a peak O<sub>3</sub> period using a single variable that is associated with or a surrogate for multiple factors that drive O<sub>3</sub> variability.

## 7. Summary and Conclusions

We found significant correlations between July MDA8 O<sub>3</sub> and select NCEP/NCAR variables for 23 monitoring sites along the Colorado Front Range and the Wasatch Front in Utah. Correlations were greatest for 500 hPa heights followed by 700 hPa temperatures, surface temperatures, and 700 hPa zonal winds, with means of 0.77, 0.75, 0.73, and –0.69, respectively. Correlations with 500 hPa heights peaked at 0.81 to 0.92 in these areas. Both include high-elevation, complex terrain and major urban centers with high precursor emissions. Analysis showed that a linear model approximates the response of O<sub>3</sub> to 500 hPa heights reasonably well. Because this variable generally produced the highest correlations, 500 hPa heights were chosen as a primary metric for this study, and regressions against 500 hPa heights were used as a tool for correcting annual trends in July MDA8 for the effects of meteorology.

Linear regressions revealed that 2002, 2003, 2006, and 2012 were high years for both July MDA8 and 500 hPa heights in Colorado and Utah. The years 1995, 1997, 2004, and 2009 were identified as low years for both O<sub>3</sub> and heights. For the high O<sub>3</sub> years, a mean high was centered in southwest Colorado and increased O<sub>3</sub> generally occurred within the upper level ridge. Significant decreases in surface scalar wind speeds were observed over the higher terrain of Colorado, Utah, and other states in the Intermountain West during the high-O<sub>3</sub>/heights years for Colorado and Utah. During the high-O<sub>3</sub>/heights period, near-normal precipitation occurred over much of the Four Corners states, but decreases were present over the Great Plains, eastern plains of Colorado, and the northern Rocky Mountain region. This pattern reversed during the low-O<sub>3</sub>/heights period. At the same time, July MDA8 for RFLAT (a high-O<sub>3</sub> site located near Denver) was significantly correlated with relative drought over much of the western U.S., but also positively correlated with a pattern of monsoon precipitation in the extreme southwestern U.S.

Differences in both 500 hPa and surface winds in Colorado between the high- and low-O<sub>3</sub>/heights cases showed a marked enhancement of easterly flows (or reduction of westerly flows), and high O<sub>3</sub> in Colorado is clearly associated with conditions favorable for well-developed mountain-plains circulations. Strong

### Acknowledgments

We would like to gratefully acknowledge the three reviewers for their valuable and constructive input. We would also like to acknowledge Frank Flocke and Mary Barth of NCAR and Brian Blaser and Daniel Bon of the Colorado Department of Public Health and Environment for their suggestions and support. Data sets used in our study were acquired from sources listed here. These include July MDA8 for available years (1995 through 2013) acquired from the Environmental Protection Agency Air Quality System (AQS) website (<http://www.epa.gov/air-data/index.html>). Hourly data for 10 July 2008 are also available at this site. Ozonesonde data for Boulder, Colorado, for 10 July 2008 were obtained from the NOAA Global Monitoring Division (<http://www.esrl.noaa.gov/gmd/dv/ftpdata.html>). The 500 hPa heights for this date were acquired from the NOAA National Operational Model Archive and Distribution System ([http://nomads.ncdc.noaa.gov/data.php?name=access#hires\\_weather\\_datasets](http://nomads.ncdc.noaa.gov/data.php?name=access#hires_weather_datasets)). Meteorological variables from two reanalysis data sets, the NCEP/NCAR Reanalysis and the NARR (<http://www.esrl.noaa.gov/psd/data/gridded/>), were provided by the NOAA Earth Systems Research Laboratory Physical Sciences Division (NOAA/OAR/ESRL PSD) in Boulder, Colorado. GPCC v6 monthly precipitation data were obtained from the Monthly/Seasonal Composites web page of the NOAA/OAR/ESRL PSD (<http://www.esrl.noaa.gov/psd/cgi-bin/data/composites/printpage.pl>), ONI ENSO index data were obtained from the NOAA/OAR/ESRL PSD (<http://www.esrl.noaa.gov/psd/data/climateindices/list>), NLDN data were obtained from the National Climatic Data Center (<https://www.ncdc.noaa.gov/data-access/severe-weather/lightning-products-and-services>), and NOAA HYSPLIT back trajectory analyses were acquired from the NOAA Air Resources Laboratory site (<http://ready.arl.noaa.gov/hypub-bin/trajtype.pl?urlr>). Correlations between July MDA8 and precipitation and PDSI data were generated using the online U.S. Climate Divisions Dataset Seasonal Correlation tool provided by NOAA/OAR/ESRL PSD (<http://www.esrl.noaa.gov/psd/data/usclimdivs/correlation/>), and Pearson correlations between measured RFLAT July MDA8 and NCEP/NCAR Reanalysis 500 hPa heights and 700 hPa zonal winds across the U.S. were plotted using a tool provided by NOAA/OAR/ESRL PSD (<http://www.esrl.noaa.gov/psd/data/correlation/>). July mean OMI tropospheric NO<sub>2</sub> data for 2005–2013 were obtained from the NASA Giovanni website [Acker and Leptoukh, 2007; [http://gdata1.sci.gsfc.nasa.gov/daac-bin/G3/gui.cgi?instance\\_id=Air\\_Quality](http://gdata1.sci.gsfc.nasa.gov/daac-bin/G3/gui.cgi?instance_id=Air_Quality)]. Colorado Front

correlations between July MDA8 and 700 hPa meridional winds in the Salt Lake City area also suggest that reduced southerly flow aloft favors enhanced terrain-driven flows and O<sub>3</sub> in the area from Salt Lake City to Provo, Utah.

We conclude that increased 500 hPa heights lead to high July O<sub>3</sub> in much of the western U.S., particularly in areas of elevated terrain near urban sources with high emissions of NO<sub>2</sub> and other O<sub>3</sub> precursors. In addition to bringing warmer temperatures, upper level ridges in this region reduce westerlies at the surface and aloft and allow cyclic terrain-driven circulations to reduce transport away from sources. Upper level ridges can also increase background concentrations within the ridge. O<sub>3</sub> and NO<sub>2</sub> concentrations build locally, and deeper vertical mixing in this region provides a potential mechanism for recapture of O<sub>3</sub> in layers aloft including urban plume residual layers, O<sub>3</sub> from thunderstorms, and O<sub>3</sub> and precursors from smoke. O<sub>3</sub> precursors and reservoir species in large-scale basin drainage flows can be brought back to source areas and nearby mountains by daytime, thermally driven upslope flows. In addition, recirculation and local accumulation can allow precursors with lower reactivities more time to contribute to local O<sub>3</sub>. Our results provide evidence that MDA8 values increase primarily because the upper level ridge is favoring processes that act on local/subregional anthropogenic emissions.

Because of the strong responses of July MDA8 and OMI tropospheric NO<sub>2</sub> to 500 hPa heights, it is not reasonable to use uncorrected trends in peak O<sub>3</sub> for much of the western U.S. for assessments of the effectiveness of emissions controls. Time series of uncorrected July MDA8 at many sites are more likely to reflect year-to-year changes in weather than changes in emissions. Robust linear regressions for July MDA8 and OMI tropospheric NO<sub>2</sub> at many sites in the western U.S. can be used to assess and correct trends in July MDA8, effectively accounting for much of the variance associated with meteorology and climatology and yielding a time series that is more directly related to trends in precursor emissions, background, and other factors. We calculated a composite time series for weather-corrected MDA8 from regressions between MDA8 and 500 hPa heights for two sets of sites: (a) 14 Front Range sites surrounding Denver and (b) nine sites surrounding Salt Lake City for 1995–2013. Corrected trends show a steady decline in O<sub>3</sub> in the Salt Lake City area but a general increase for the Front Range since 2004, broken only by the recession of late 2008. The method for accounting for the effects of weather presented here could be of particular value to state, local, and federal air quality managers who are tasked with assessing the effectiveness of control strategies over time and the impacts of sources beyond their jurisdiction. The method we have described uses readily available data, is simple, and identifies patterns and signals specific to a peak O<sub>3</sub>.

### References

- Acker, J. G., and G. Leptoukh (2007), Online analysis enhances use of NASA Earth Science Data, *Eos Trans. AGU*, 88(2), 14–17.
- Adams, D. K., and A. C. Comrie (1997), The North American monsoon, *Bull. Am. Meteorol. Soc.*, 78(10), 2197–2213, doi:10.1175/1520-0477(1997)078<2197:TNA>2.0.CO;2.
- Becker, A., P. Finger, A. Meyer-Christoffer, B. Rudolf, K. Schamm, U. Schneider, and M. Ziese (2013), A description of the global land-surface precipitation data products of the Global Precipitation Climatology Centre with sample applications including centennial (trend) analysis from 1901–present, *Earth Syst. Sci. Data*, 5(1), 71–99, doi:10.5194/essd-5-71-2013.
- Bertschi, I. T., and D. A. Jaff (2005), Long-range transport of ozone, carbon monoxide, and aerosols to the NE Pacific troposphere during the summer of 2003: Observations of smoke plumes from Asian boreal fires, *J. Geophys. Res.*, 110, D05303, doi:10.1029/2004JD005135.
- Bloomer, B. J., J. W. Stehr, C. A. Piety, R. J. Salawitch, and R. R. Dickerson (2009), Observed relationships of ozone air pollution with temperature and emissions, *Geophys. Res. Lett.*, 36, L09803, doi:10.1029/2009GL037308.
- Bossert, J. E., and W. R. Cotton (1994a), Regional-scale flows in mountainous terrain. Part I: A numerical and observational comparison, *Mon. Weather Rev.*, 122(7), 1449–1471.
- Bossert, J. E., and W. R. Cotton (1994b), Regional-scale flows in mountainous terrain. Part II: Simplified numerical experiments, *Mon. Weather Rev.*, 122(7), 1472–1489, doi:10.1175/1520-0493(1994)122<1472:RSFIMT>2.0.CO;2.
- Bossert, J. E., J. D. Sheaffer, and E. R. Reiter (1989), Aspects of regional-scale flows in mountainous terrain, *J. Appl. Meteorol.*, 28(7), 590–601, doi:10.1175/1520-0450(1989)028<0590:AORSFI>2.0.CO;2.
- Bucsela, E. J., N. A. Krotkov, E. A. Celarier, L. N. Lamsal, W. H. Swartz, P. K. Bhartia, K. F. Boersma, J. P. Veefkind, J. F. Gleason, and K. E. Pickering (2013), A new stratospheric and tropospheric NO<sub>2</sub> retrieval algorithm for nadir-viewing satellite instruments: Applications to OMI, *Atmos. Meas. Tech.*, 6(10), 2607–2626, doi:10.5194/amt-6-2607-2013.
- Camalier, L., W. Cox, and P. Dolwick (2007), The effects of meteorology on ozone in urban areas and their use in assessing ozone trends, *Atmos. Environ.*, 41, 7127–7137, doi:10.1016/j.atmosenv.2007.04.061.
- Cleveland, W. S. (1979), Robust locally weighted regression and smoothing scatterplots, *J. Am. Stat. Assoc.*, 74(368), 829–836, doi:10.1080/01621459.1979.10481038.
- Colorado Department of Local Affairs (2015), Population totals for Colorado and sub-state regions. [Available at <https://www.colorado.gov/pacific/dola/node/104461>.]
- Cooper, O. R., et al. (2007), Evidence for a recurring eastern North America upper tropospheric ozone maximum during summer, *J. Geophys. Res.*, 112, D23304, doi:10.1029/2007JD008710.

Range population data were acquired from the Colorado Department of Local Affairs (<https://www.colorado.gov/pacific/dola/node/104461>). The regional climate simulation work was supported by NSF-EaSM grant AGS-1048829 "Developing a Next-Generation Approach to Regional Climate Prediction at High Resolution." Model simulations were made possible by an NCAR Accelerated Scientific Discovery (ASD) grant. NCAR is operated by the University Corporation of Atmospheric Research under sponsorship of the National Science Foundation. This research was also supported in part by the NASA AQAST project (grant NNX11AI51G).

- Cooper, O. R., R.-S. Gao, D. Tarasick, T. Leblanc, and C. Sweeney (2012), Long-term ozone trends at rural ozone monitoring sites across the United States, 1990–2010, *J. Geophys. Res.*, 117, D22307, doi:10.1029/2012JD018261.
- Davis, J., W. Cox, A. Reff, and P. Dolwick (2011), A comparison of CMAQ-based and observation-based statistical models relating ozone to meteorological parameters, *Atmos. Environ.*, 45(20), 3481–3487, doi:10.1016/j.atmosenv.2010.12.060.
- Done, J., G. Holland, C. Bruyère, L. R. Leung, and A. Suzuki-Parker (2013), Modeling high-impact weather and climate: Lessons from a tropical cyclone perspective, *Clim. Change*, 1–15, doi:10.1007/s10584-013-0954-6.
- Dosio, A., Galmarini S., and Graziani G. (2002), Simulation of the circulation and related photochemical ozone dispersion in the Po plains (northern Italy): Comparison with the observations of a measuring campaign, *J. Geophys. Res.*, 107(D22), 8189, doi:10.1029/2000JD000046.
- Draxler, R., and G. Rolph (2014), HYSPLIT (HYbrid Single-Particle Lagrangian Integrated Trajectory) model access via NOAA ARL READY website. [Available at <http://www.arl.noaa.gov/HYSPLIT.php> NOAA Air Resources Laboratory, College Park, MD.]
- Ek, M. B., and A. A. M. Holtslag (2004), Influence of soil moisture on boundary layer cloud development, *J. Hydrometeorol.*, 5(1), 86–99, doi:10.1175/1525-7541(2004)005<0086:IOSMOB>2.0.CO;2.
- Ellis, A. W., M. L. Hildebrandt, W. M. Thomas, and H. J. Fernando (2000), Analysis of the climatic mechanisms contributing to the summertime transport of lower atmospheric ozone across metropolitan Phoenix, Arizona, USA, *Clim. Res.*, 15(1), 13–31.
- Eskridge, R. E., J. Y. Ku, S. T. Rao, P. S. Porter, and I. G. Zurbenko (1997), Separating different scales of motion in time series of meteorological variables, *Bull. Am. Meteorol. Soc.*, 78(7), 1473–1483.
- Henne, S., M. Furger, S. Nyeki, M. Steinbacher, B. Neininger, S. F. J. De Wekker, J. Dommen, N. Spichtinger, A. Stohl, and A. S. H. Prévôt (2004), Quantification of topographic venting of boundary layer air to the free troposphere, *Atmos. Chem. Phys.*, 4(2), 497–509.
- Jaffe, D. A., and N. L. Wigder (2012), Ozone production from wildfires: A critical review, *Atmos. Environ.*, 51, 1–10, doi:10.1016/j.atmosenv.2011.11.063.
- Jaffe, D., I. Bertschi, L. Jaeglé, P. Novelli, J. S. Reid, H. Tanimoto, R. Vingarzan, and D. L. Westphal (2004), Long-range transport of Siberian biomass burning emissions and impact on surface ozone in western North America, *Geophys. Res. Lett.*, 31, L16106, doi:10.1029/2004GL020093.
- Jaffe, D., D. Chand, W. Hafner, A. Westerling, and D. Spracklen (2008), Influence of fires on O<sub>3</sub> concentrations in the western U.S., *Environ. Sci. Technol.*, 42(16), 5885–5891, doi:10.1021/es800084k.
- Kalnay, E., et al. (1996), The NCEP/NCAR 40-year reanalysis project, *Bull. Am. Meteorol. Soc.*, 77(3), 437–471, doi:10.1175/1520-0477(1996)077<0437:TNYRP>2.0.CO;2.
- Lamarque, J.-F., G. P. Kyle, M. Meinshausen, K. Riahi, S. Smith, D. van Vuuren, A. Conley, and F. Vitt (2011), Global and regional evolution of short-lived radiatively-active gases and aerosols in the Representative Concentration Pathways, *Clim. Change*, 109(1–2), 191–212, doi:10.1007/s10584-011-0155-0.
- Lamsal, L. N., et al. (2014), Evaluation of OMI operational standard NO<sub>2</sub> column retrievals using in situ and surface-based NO<sub>2</sub> observations, *Atmos. Chem. Phys.*, 14(21), 11,587–11,609, doi:10.5194/acp-14-11587-2014.
- Langford, A. O., C. J. Senff, R. J. Alvarez, R. M. Banta, and R. M. Hardesty (2010), Long-range transport of ozone from the Los Angeles Basin: A case study, *Geophys. Res. Lett.*, 37, L06807, doi:10.1029/2010GL042507.
- MacDonald, C. P., P. T. Roberts, H. H. Main, T. S. Dye, D. L. Coe, and J. Yarbrough (2001), The 1996 Paso del Norte Ozone Study: Analysis of meteorological and air quality data that influence local ozone concentrations, *US-Mex. Transbound. Air Pollut. Stud.*, 276(1–3), 93–109, doi:10.1016/S0048-9697(01)00774-4.
- McKendry, I. G., and J. Lundgren (2000), Tropospheric layering of ozone in regions of urbanized complex and/or coastal terrain: A review, *Prog. Phys. Geogr.*, 24(3), 329–354.
- Mesinger, F., et al. (2006), North American Regional Reanalysis, *Bull. Am. Meteorol. Soc.*, 87(3), 343–360, doi:10.1175/BAMS-87-3-343.
- Milanchus, M. L., S. T. Rao, and I. G. Zurbenko (1998), Evaluating the effectiveness of ozone management efforts in the presence of meteorological variability, *J. Air Waste Manage. Assoc.*, 48(3), 201–215.
- Musselman, R. C., and J. L. Korfmacher (2014), Ozone in remote areas of the Southern Rocky Mountains, *Atmos. Environ.*, 82, 383–390, doi:10.1016/j.atmosenv.2013.10.051.
- Pan, H.-L., and L. Mahrt (1987), Interaction between soil hydrology and boundary-layer development, *Bound. Layer Meteorol.*, 38(1–2), 185–202, doi:10.1007/BF00121563.
- Pan, L. L., et al. (2014), Thunderstorms enhance tropospheric ozone by wrapping and shedding stratospheric air, *Geophys. Res. Lett.*, 41, 7785–7790, doi:10.1002/2014GL061921.
- Pétron, G., et al. (2014), A new look at methane and nonmethane hydrocarbon emissions from oil and natural gas operations in the Colorado Denver-Julesburg Basin, *J. Geophys. Res. Atmos.*, 119, 6836–6852, doi:10.1002/2013JD021272.
- Pfister, G. G., S. Walters, J.-F. Lamarque, J. Fast, M. C. Barth, J. Wong, J. Done, G. Holland, and C. L. Bruyère (2014), Projections of future summertime ozone over the U.S.: Projections of future U.S. surface ozone, *J. Geophys. Res. Atmos.*, 119, 5559–5582, doi:10.1002/2013JD020932.
- Porter, P. S., S. T. Rao, I. G. Zurbenko, A. M. Dunker, and G. T. Wolff (2001), Ozone air quality over North America: Part II—An analysis of trend detection and attribution techniques, *J. Air Waste Manage. Assoc.*, 51(2), 283–306.
- Rasmussen, D. J., A. M. Fiore, V. Naik, L. W. Horowitz, S. J. McGinnis, and M. G. Schultz (2012), Surface ozone-temperature relationships in the eastern U.S.: A monthly climatology for evaluating chemistry-climate models, *Atmos. Environ.*, 47, 142–153, doi:10.1016/j.atmosenv.2011.11.021.
- Reddy, P. J., D. E. Barbarick, and R. D. Osterburg (1995), Development of a statistical model for forecasting episodes of visibility degradation in the Denver metropolitan area, *J. Appl. Meteorol.*, 34(3), 616–625, doi:10.1175/1520-0450(1995)034<0616:DOASMF>2.0.CO;2.
- Rolph, G. D. (2014), Real-time Environmental Applications and Display sYstem (READY) website. [Available at <http://www.ready.noaa.gov>. NOAA Air Resources Laboratory, College Park, MD.]
- Russell, A. R., L. C. Valin, and R. C. Cohen (2012), Trends in OMI NO<sub>2</sub> observations over the United States: Effects of emission control technology and the economic recession, *Atmos. Chem. Phys.*, 12(24), 12,197–12,209, doi:10.5194/acp-12-12197-2012.
- Schneider, U., A. Becker, P. Finger, A. Meyer-Christoffer, B. Rudolf, and M. Ziese (2011), GPCC full data reanalysis version 6.0 at 0.5°: Monthly land-surface precipitation from rain-gauges built on GTS-based and historic data.
- Schneider, U., A. Becker, P. Finger, A. Meyer-Christoffer, M. Ziese, and B. Rudolf (2014), GPCC's new land surface precipitation climatology based on quality-controlled in situ data and its role in quantifying the global water cycle, *Theor. Appl. Climatol.*, 115(1–2), 15–40, doi:10.1007/s00704-013-0860-x.
- Seidel, D. J., Y. Zhang, A. Beljaars, J.-C. Golaz, A. R. Jacobson, and B. Medeiros (2012), Climatology of the planetary boundary layer over the continental United States and Europe: Boundary layer climatology: U.S. and Europe, *J. Geophys. Res.*, 117, D17106, doi:10.1029/2012JD018143.

- Sillman, S., and P. J. Samson (1995), Impact of temperature on oxidant photochemistry in urban, polluted rural and remote environments, *J. Geophys. Res.*, 100, 11,497–11,508, doi:10.1029/94JD02146.
- Steiner, A. L., A. J. Davis, S. Sillman, R. C. Owen, A. M. Michalak, and A. M. Fiore (2010), Observed suppression of ozone formation at extremely high temperatures due to chemical and biophysical feedbacks, *Proc. Natl. Acad. Sci. U.S.A.*, 107(46), 19,685–19,690.
- Stewart, J. Q., C. D. Whiteman, W. J. Steenburgh, and X. Bian (2002), A climatological study of thermally driven wind systems of the U.S. intermountain west, *Bull. Am. Meteorol. Soc.*, 83(5), 699–708, doi:10.1175/1520-0477(2002)083<0699:ACSOTD>2.3.CO;2.
- Szoke, E. J. (1991), Eye of the Denver cyclone, *Mon. Weather Rev.*, 119(5), 1283–1292, doi:10.1175/1520-0493(1991)119<1283:EOTDC>2.0.CO;2.
- Szoke, E. J., and J. A. Augustine (1990), An examination of the mean flow and thermodynamic characteristics of a mesoscale flow feature: the Denver cyclone, in *Preprints, Fourth Conference on Mesoscale Processes*, pp. J17–J18, American Meteorological Society, Boulder, CO.
- Tawfik, A. B., and A. L. Steiner (2013), A proposed physical mechanism for ozone-meteorology correlations using land-atmosphere coupling regimes, *Atmos. Environ.*, 72, 50–59, doi:10.1016/j.atmosenv.2013.03.002.
- Tong, D. Q., L. Lamsal, L. Pan, C. Ding, H. Kim, P. Lee, T. Chai, K. E. Pickering, and I. Stajner (2015), Long-term NO<sub>x</sub> trends over large cities in the United States during the great recession: Comparison of satellite retrievals, ground observations, and emission inventories, *Atmos. Environ.*, 107, 70–84, doi:10.1016/j.atmosenv.2015.01.035.
- Toth, J. J., and R. H. Johnson (1985), Summer surface flow characteristics over northeast Colorado, *Mon. Weather Rev.*, 113(9), 1458–1469, doi:10.1175/1520-0493(1985)113<1458:SSFCON>2.0.CO;2.
- White, A. B., L. S. Darby, C. J. Senff, C. W. King, R. M. Banta, J. Koerner, J. M. Wilczak, P. J. Neiman, W. M. Angevine, and R. Talbot (2007), Comparing the impact of meteorological variability on surface ozone during the NEAQS (2002) and ICARTT (2004) field campaigns, *J. Geophys. Res.*, 112, D10S14, doi:10.1029/2006JD007590.
- Wiedinmyer, C., S. K. Akagi, R. J. Yokelson, L. K. Emmons, J. A. Al-Saadi, J. J. Orlando, and A. J. Soja (2011), The Fire INventory from NCAR (FINN): A high resolution global model to estimate the emissions from open burning, *Geosci. Model Dev.*, 4(3), 625–641, doi:10.5194/gmd-4-625-2011.
- Wise, E., and A. Comrie (2005), Meteorologically adjusted urban air quality trends in the southwestern United States, *Atmos. Environ.*, 39(16), 2969–2980, doi:10.1016/j.atmosenv.2005.01.024.
- Wolyn, P. G., and T. B. McKee (1994), The mountain-plains circulation east of a 2-km-high north-south barrier, *Mon. Weather Rev.*, 122(7), 1490–1508, doi:10.1175/1520-0493(1994)122<1490:TMPCCEO>2.0.CO;2.
- Zhang, J., and S. T. Rao (1999), The role of vertical mixing in the temporal evolution of ground-level ozone concentrations, *J. Appl. Meteorol.*, 38(12), 1674–1691.
- Zhang, L., D. J. Jacob, X. Yue, N. V. Downey, D. A. Wood, and D. Blewitt (2014a), Sources contributing to background surface ozone in the US Intermountain West, *Atmos. Chem. Phys.*, 14(11), 5295–5309, doi:10.5194/acp-14-5295-2014.
- Zhang, X., S. Kondragunta, and D. P. Roy (2014b), Interannual variation in biomass burning and fire seasonality derived from geostationary satellite data across the contiguous United States from 1995 to 2011, *J. Geophys. Res. Biogeosci.*, 119, 1147–1162, doi:10.1002/2013JG002518.
- Zhou, X., and B. Geerts (2012), The influence of soil moisture on the planetary boundary layer and on cumulus convection over an isolated mountain. Part I: Observations, *Mon. Weather Rev.*, 141(3), 1061–1078, doi:10.1175/MWR-D-12-00150.1.